DOI: 10.1002/chem.200501067

Guest-Dependent Flexible Coordination Networks with Fluorinated Ligands

Kayoko Kasai*[a] and Makoto Fujita[b]

Abstract: Guest-dependent flexible coordination networks are formed from 1,4-bis(4-pyridylmethyl)tetrafluorobenzene (bpf), 4,4′-bis(4-pyridylmethyl)octafluorobiphenyl (bpfb), 2,6-bis(4-pyridylmethyl)hexafluoronaphthalene (2,6-bpfn), and 2,7-bis(4-pyridylmethyl)hexafluoronaphthalene (2,7-bpfn) with $Cd(NO_3)_2$ in the presence of various organic compounds. The reaction of bpf affords one-dimensional cyclic chains, two-dimensional rhombus grid sheets, and three-dimensional diamond frameworks with threefold interpenetration. The reaction of bpfb mainly affords two-dimensional rhombus grid sheets with twofold parallel interpenetration. The reaction of 2,6-bpfn affords a one-dimensional ladder and two-dimensional rhombus grid, twisted grid, and herringbone sheets. The reaction of 2,7-bpfn affords two-dimensional rhombus grid sheets and grid sheets with dumbbell-shaped cavities. This diversity of network topologies is induced by interactions between the guest molecules and the flexible ligand frameworks.

Keywords: coordination networks · crystal engineering · host–guest systems · N ligands · supramolecular chemistry

Introduction

Infinite coordination networks derived from metal ions and bridging ligands have attracted much attention in recent years due to the challenge of constructing novel metal–ligand architectures[1,2] as well as their potential in applications such as optical,[3] magnetic,[4] electronic,[5] and porous materials.[6] In particular, coordination networks with inner cavities and channels capable of clathrating guest species are of interest as zeolite-like materials for gas adsorption,[7] chemical adsorption,[8] ion-exchange,[9] and heterogeneous catalysis.[10] Their well-defined hydrophobic cavities and channels surrounded by organic components are important for specific functions, and key factors for success in fabricating such materials are the selection and combination of metal ions and bridging ligands.

We have reported the first typical coordination zeolite $[Cd(bipy)_2(NO_3)_2]_n$, which is prepared from the rod-like bidentate ligand 4,4′-bipyridine (bipy) and $Cd(NO_3)_2$.[10a] The two-dimensional square grid network has functions including selective heterogeneous catalysis and separation of isomers such as those of dichlorobenzene and dibromobenzene. Kitagawa and Kondo et al. have reported the preparation of a series of $[M_2(bipy)_3(NO_3)_4]_n$ complexes ($M = Co^{II}$, Ni^{II}, Zn^{II}) that show reversible adsorption/desorption of gases such as CH_4, N_2, CO_2, and Ar.[7a] These networks have tongue-and-groove structures in which two-dimensional bilayer frameworks pack by partial interdigitation and one-dimensional channels run through the structures. Yaghi et al. have reported the synthesis of charge-neutral porous coordination networks containing multitopic benzenecarboxylates as building blocks, in which aromatic solvents may be selectively included.[8a,c]

The design of multidentate bridging ligands is a predominant factor in determining the structures and functions of coordination networks. The bipyridine network $[Cd(bipy)_2(NO_3)_2]_n$, for example, can form a clathrate complex with *o*-dihalobenzenes but not with *m*- or *p*-dihalobenzenes.[10a] This high selectivity, which is based on the size- and shape-specificity of the inner cavity, may be attributed to the rigidity of the bidentate bipy ligand and the octahedral coordination geometry of the Cd^{II} ion, with four pyridine rings at the equatorial positions and two monodentate nitrate anions at the axial positions. In the aromatic carboxylate network $\{[CoC_6H_3(COOH_{1/3})_3(py)_2]\cdot 2/3py\}_n$, the solid material can selectively adsorb aromatic molecules such as benzo-

[a] Dr. K. Kasai
Miyagi University of Education
149 Aoba, Aramaki, Aoba-ku 980-0845 Sendai (Japan)
Fax: (+41) 22-214-3429
E-mail: kasai@staff.miyakyo-u.ac.jp

[b] Prof. Dr. M. Fujita
Department of Applied Chemistry, School of Engineering
The University of Tokyo, Hongo, Bunkyo-ku 113-8656 Tokyo (Japan)

Supporting Information for this article is available on the WWW under http://www.chemeurj.org/ or from the author.

nitrile, nitrobenzene, and chlorobenzene but not acetonitrile, nitromethane, or dichloroethane.[8a] This remarkable selectivity results from the combination of a rigid tridentate ligand (1,3,5-benzenetricarboxylate) and a spacer unit of anchored pyridine, in which the layers are held tightly together by mutual π stacking.

The use of such rigid ligands allows selective enclathration of guest organic compounds with size- and shape-specificity. In contrast to rigid ligands, flexible ligands with conformational freedom have significant potential for forming the basis of coordination networks with a large variety of structures and topologies. Zaworotko et al. have reported the occurrence of supramolecular isomerism in coordination networks with the flexible ligand 1,2-bis(4-pyridyl)ethane (bpe).[11] Its complex with $Co(NO_3)_2$ can afford 1D rod-to-ring chains, bilayers, or ladder arrays with identical molecular formulae $[Co(bpe)_{1.5}(NO_3)_2]$ and asymmetric units. The supramolecular isomerism results from *gauche* or *anti* conformations of the bpe ligand. Stang et al. have reported an assortment of different structures with a single metal-ligand system using 1,3-bis(4-pyridyl)propane as ligand.[12] The supramolecular topologies are dependent on simple organic guests such as benzene, toluene, or *cis*-stilbene to afford closed dinuclear macrocycles and infinite helical and wedge-shaped one-dimensional networks. The network structures are influenced by intermolecular host–guest and/or guest–guest interactions.

The introduction of electron-deficient substituents into the ligand framework is one of the most promising methods to improve the enclathration ability of coordination networks with electron-rich aromatic ring compounds because of the efficient intermolecular interactions between aromatic and fluorinated aromatic rings. Based on this concept, we have designed and prepared the fluorinated flexible ligands 1,4-bis(4-pyridylmethyl)tetrafluorobenzene (bpf), 4,4′-bis(4-pyridylmethyl)octafluorobiphenyl (bpfb), 2,6-bis(4-pyridylmethyl)hexafluoronaphthalene (2,6-bpfn), and 2,7-bis(4-pyridylmethyl)hexafluoronaphthalene (2,7-bpfn), in which two pyridylmethyl groups are bridged by perfluoroaromatic rings[8e,13] (Scheme 1). Herein, we report a comprehensive overview of the metal–ligand network architectures with fluorinated flexible backbones in which the coordination networks contain guest organic molecules derived from the fluorinated ligands, $Cd(NO_3)_2$,[1m] and various aromatic compounds.

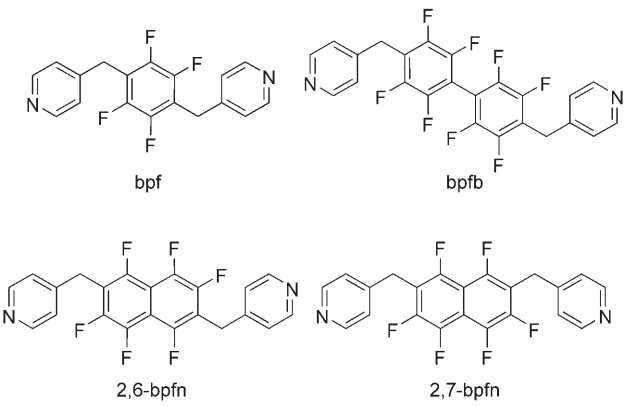

Scheme 1. The fluorinated flexible ligands bpf, bpfb, 2,6-bpfn, and 2,7-bpfn.

Results and Discussion

We used various combinations of $Cd(NO_3)_2$, fluorinated flexible ligand (bpf, bpfb, 2,6-bpfn and 2,7-bpfn), and aromatic compounds in H_2O:EtOH (1:4), and obtained nearly forty coordination networks in satisfactory yields (19–73%). All of them were characterized by single-crystal X-ray diffraction analysis.

The reactions with bpf resulted in the formation of many types of host framework whose network topologies vary significantly depending on slight differences in the structures of the guest molecules. They include 1) a 1D chain network composed of a cyclic linkage with stoichiometry $ML_2{\cdot}G$ (**1a**, **b**), 2) 2D grid networks with stoichiometries $ML_2{\cdot}G$ (**2a–d**), $ML_2{\cdot}G_2$ (**3**), $ML_2{\cdot}G_3$ (**4**), and $ML_2{\cdot}G_4$ (**5a**, **b**), and 3) a 3D diamond network with stoichiometry $ML_2{\cdot}G_2$ (**6a–h**). The 2D grid structures are relatively common host frameworks that appear throughout our experiments. The cavity in the grid network is composed of four metal ions and four ligands, which form a rhombus-like shape. Remarkably, the 2D grid sheets can swell when the number of guest molecules per cavity increases. The reactions with bpfb afforded 2D grid structures that incorporate two guest compound molecules in each cavity and have the stoichiometry $ML_2{\cdot}G_2$ (**7**, **8a–e**). The reactions with 2,6-bpfn afforded a 1D ladder with stoichiometry $ML_{1.5}{\cdot}G$ (**9**) and three types of 2D networks, namely a 2D rhombus grid with stoichiometry $ML_2{\cdot}G_2$ (**10a–c**), a twisted 2D thick grid with stoichiometry $ML_2{\cdot}G_2$ (**11a–g**), and a 2D herringbone pattern with stoichiometry $M_2L_3{\cdot}G$ (**12**). In contrast, 2,7-bpfn, which is a regioisomer of 2,6-bpfn, afforded two types of 2D structures with stoichiometry $ML_2{\cdot}G_2$, namely a 2D rhombus grid (**13**) and a 2D rhombus grid with dumbbell-shaped cavities (**14a**, **b**). These networks are summarized in Scheme 2.

$\{[Cd(bpf)_2(NO_3)_2]{\cdot}Ph\mathit{t}Bu\}_n$ (1a): The coordination geometry of **1a** is shown in Figure 1a as a typical example. Two crystallographically independent cadmium ions adopt an octahedral geometry with four bpf pyridine rings at the equatorial positions and two monodentate NO_3^- anions at the axial positions. Both ligands adopt *cis* conformations to form a cyclic framework. The extended structure forms a polymeric 1D chain network by infinite linking of boat-shaped cyclic frameworks (Figure 1b). The adjacent Cd^{II} ions are bridged by two *cis* ligands with a distance of 12.15 Å, and one guest molecule of *tert*-butylbenzene is packed into each cyclic cavity. The cyclic shape is suitable for a guest aromatic compound with a bulky substituent; the benzene ring of the guest molecule is packed between two bpf pyridine rings, while the opposite side of the cavity is spacious enough for the bulky *tert*-butyl group. The aromatic ring of the guest

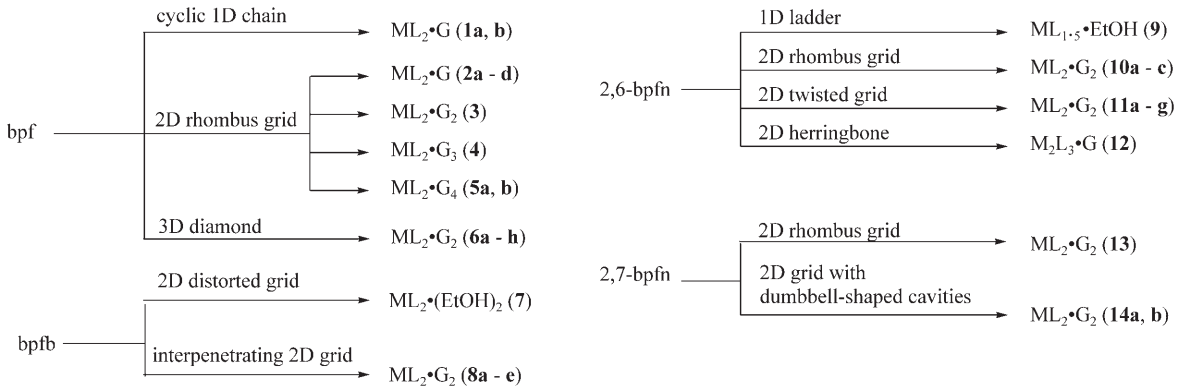

{[Cd(bpf)$_2$(NO$_3$)$_2$]•Ph*t*Bu}$_n$ **1a**
{[Cd(bpf)$_2$(NO$_3$)$_2$]•PhCHMe$_2$}$_n$ **1b**
{[Cd(bpf)$_2$(NO$_3$)$_2$]•PhNMe$_2$}$_n$ **2a**
{[Cd(bpf)$_2$(NO$_3$)$_2$]•*p*-C$_6$H$_4$Me$_2$}$_n$ **2b**
{[Cd(bpf)$_2$(NO$_3$)$_2$]•*o*-C$_6$H$_4$BrOMe}$_n$ **2c**
{[Cd(bpf)$_2$(NO$_3$)$_2$]•naphthalene}$_n$ **2d**
{[Cd(bpf)$_2$(NO$_3$)$_2$]•(*p*-C$_6$H$_4$BrMe)$_2$}$_n$ **3**
{[Cd(bpf)$_2$(NO$_3$)$_2$]•(C$_6$H$_6$)$_3$}$_n$ **4**
{[Cd(bpf)$_2$(NO$_3$)$_2$]•(*o*-C$_6$H$_4$Me$_2$)$_4$}$_n$ **5a**
{[Cd(bpf)$_2$(NO$_3$)$_2$]•(*o*-C$_6$H$_4$NH$_2$Me)$_4$}$_n$ **5b**
{[Cd(bpf)$_2$(NO$_3$)$_2$]•(PhOCOMe)$_2$}$_n$ **6a**
{[Cd(bpf)$_2$(NO$_3$)$_2$]•(*m*-C$_6$H$_4$Me$_2$)$_2$}$_n$ **6b**
{[Cd(bpf)$_2$(NO$_3$)$_2$]•(PhNHMe)$_2$}$_n$ **6c**
{[Cd(bpf)$_2$(NO$_3$)$_2$]•(PhMe)$_2$}$_n$ **6d**
{[Cd(bpf)$_2$(NO$_3$)$_2$]•(biphenyl)$_2$}$_n$ **6e**
{[Cd(bpf)$_2$(NO$_3$)$_2$]•(PhCH$_2$OMe)$_2$}$_n$ **6f**
{[Cd(bpf)$_2$(NO$_3$)$_2$]•(PhEt)$_2$}$_n$ **6g**
{[Cd(bpf)$_2$(NO$_3$)$_2$]•(PhCH(Me)=CH$_2$)$_2$}$_n$ **6h**
{[Cd(bpfb)$_2$(NO$_3$)$_2$]•(EtOH)$_2$}$_n$ **7**
{[Cd(bpfb)$_2$(NO$_3$)$_2$]•(PhOCOMe)$_2$}$_n$ **8a**
{[Cd(bpfb)$_2$(NO$_3$)$_2$]•(PhNMe$_2$)$_2$}$_n$ **8b**
{[Cd(bpfb)$_2$(NO$_3$)$_2$]•(*m*-C$_6$H$_4$(OMe)$_2$)$_2$}$_n$ **8c**
{[Cd(bpfb)$_2$(NO$_3$)$_2$]•(biphenyl)$_2$}$_n$ **8d**
{[Cd(bpfb)$_2$(NO$_3$)$_2$]•(naphthalene)$_2$}$_n$ **8e**
{[Cd(2,6-bpfn)$_{1.5}$(NO$_3$)$_2$]•EtOH}$_n$ **9**
{[Cd(2,6-bpfn)$_2$(NO$_3$)$_2$]•(*p*-C$_6$H$_4$(OMe)$_2$)$_2$}$_n$ **10a**
{[Cd(2,6-bpfn)$_2$(NO$_3$)$_2$]•(PhCOOMe)$_2$}$_n$ **10b**
{[Cd(2,6-bpfn)$_2$(NO$_3$)$_2$]•(biphenyl)$_2$}$_n$ **10c**
{[Cd(2,6-bpfn)$_2$(NO$_3$)$_2$]•(*p*-C$_6$H$_4$Me$_2$)$_2$}$_n$ **11a**
{[Cd(2,6-bpfn)$_2$(NO$_3$)$_2$]•(naphthalene)$_2$}$_n$ **11b**
{[Cd(2,6-bpfn)$_2$(NO$_3$)$_2$]•(*m*-C$_6$H$_4$Me$_2$)$_2$}$_n$ **11c**
{[Cd(2,6-bpfn)$_2$(NO$_3$)$_2$]•(*m*-C$_6$H$_4$(OMe$_2$)$_2$}$_n$ **11d**
{[Cd(2,6-bpfn)$_2$(NO$_3$)$_2$]•(PhNMe$_2$)$_2$}$_n$ **11e**
{[Cd(2,6-bpfn)$_2$(NO$_3$)$_2$]•(*p*-C$_6$H$_4$BrMe)$_2$}$_n$ **11f**
{[Cd(2,6-bpfn)$_2$(NO$_3$)$_2$]•(PhCH(Me)=CH$_2$)$_2$}$_n$ **11g**
{[Cd$_2$(2,6-bpfn)$_3$(NO$_3$)$_4$]•PhNHMe}$_n$ **12**
{[Cd(2,7-bpfn)$_2$(NO$_3$)$_2$]•(*m*-C$_6$H$_4$(OMe)$_2$)$_2$}$_n$ **13**
{[Cd(2,7-bpfn)$_2$(NO$_3$)$_2$]•(*m*-C$_6$H$_4$Me$_2$)$_2$}$_n$ **14a**
{[Cd(2,7-bpfn)$_2$(NO$_3$)$_2$]•(PhOCOMe)$_2$}$_n$ **14b**

Scheme 2. Preparation of **1a**, **b**, **2a–d**, **3**, **4**, **5a**, **5b**, **6a–h**, **7**, **8a–e**, **9**, **10a–c**, **11a–g**, **12**, **13**, **14a**, and **14b**.

molecule is packed between two pyridine rings by an edge-to-face interaction with an edge-tiled T-shaped structure. The H2A···C39 and H35A···C41 distances are 2.938 and 2.978 Å, respectively (Figure 1d). A side view of the chains is shown in Figure 1c. These zig-zag 1D coordination polymers are linked by hydrogen bonds to form a 2D flat layer. Either coordinating or noncoordinating oxygen atoms of nitrate anions bind to the methylene groups of both the neighboring chains (N5–O1···H13B 2.429, N5–O3···H31A 2.439, N6–O4···H24B 2.442, N6–O6···H6A 2.385 Å). The guest aromatic rings are linked by C–H···F hydrogen bonds with neighboring chains. The H39A···F7 and H41A···F2 distances are 2.734 and 2.675 Å, respectively. These layers are stacked parallel to each other through C–H···F hydrogen bonds (H6B···F1 2.458, H15A···F3 2.587, H24A···F6 2.743, H31B···F8 2.386 Å), as shown in Figure 1e.

{[Cd(bpf)$_2$(NO$_3$)$_2$]·PhNMe$_2$}$_n$ (2a): The coordination environment of Cd^{II} in **2a** is octahedral, similar to that of **1a**. The crystal structure of **2a** belongs to the space group $P\bar{1}$ and contains half of a Cd(NO$_3$)$_2$ moiety, a bpf molecule, and half of an *N*,*N*-dimethylaniline molecule per unit cell. The sheet structure is shown in Figure 2a. All the ligands adopt *trans* conformations, in contrast to the *cis* conformations found in the 1D chain structures of **1a** and **1b**. The network topology is a 2D rhombus grid in which the diagonal-to-diagonal distances and dimensions are 29.79×13.11 and 16.87×15.64 Å, respectively. Each cavity surrounded by four Cd^{II} ions and four ligands contains one molecule of *N*,*N*-dimethylaniline. The aromatic ring of *N*,*N*-dimethylaniline is packed between two pyridine rings by edge-to-face interactions. The H4A···centroid distance is 2.499 Å (Figure 2a). The 2D sheet is relatively flat and is made into layers stacked on each other with an interplanar distance of 5.3 Å linked by two types of hydrogen bonds. The N3–O3···H12A and H11A···F3 distances are 2.462 and 2.517 Å, respectively (Figure 2b). Moreover, the guest molecules are linked by C–H···F hydrogen bonds with neighboring sheets (H20A···F4 2.638, H24A···F4 2.284 Å), as shown in Figure 2c. The *p*-xylene clathrated network **2b** is isostructural with **2a** and has the same space group.

{[Cd(bpf)$_2$(NO$_3$)$_2$]·*o*-C$_6$H$_4$BrOMe}$_n$ (2c): The structure of **2c** is analogous to that of **2a** except that it is about twice the length along the *c* axis (**2a**: $c=10.717(5)$; **2c**: $c=21.438(4)$ Å). Consequently, the unit cell is composed of Cd-

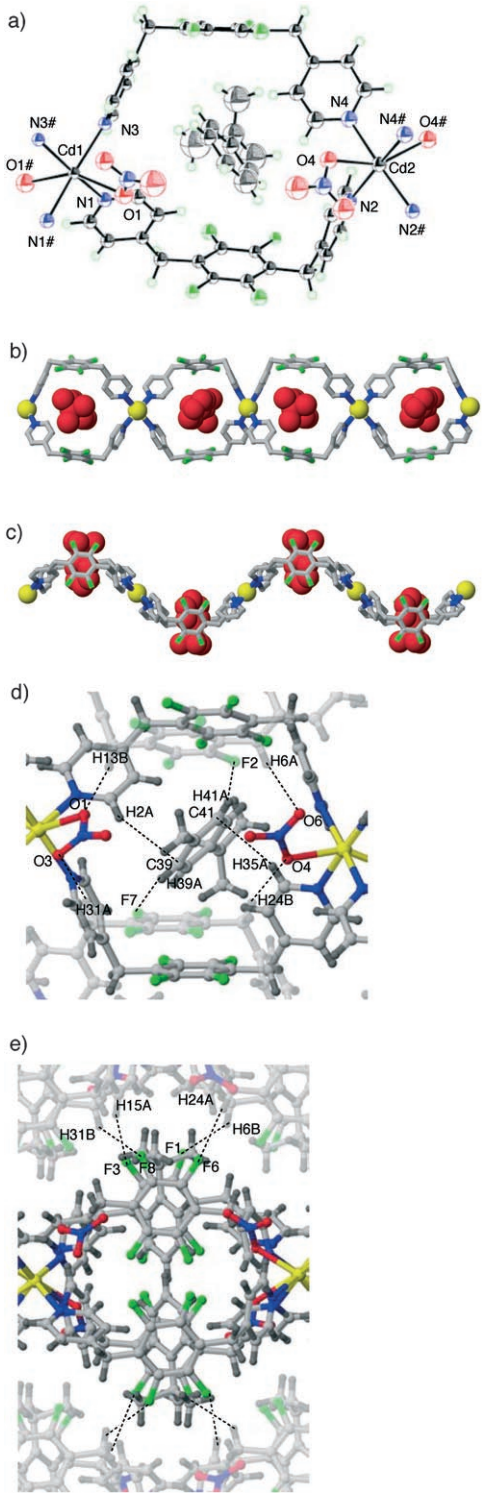

Figure 1. Crystal structure of **1a**: a) ORTEP view around the metal center (thermal ellipsoid probability: 50%); b) top view of the 1D chain; c) side view of the 1D chain; d) top view of the packing of a cyclic cavity; e) side view of the packing of the layers.

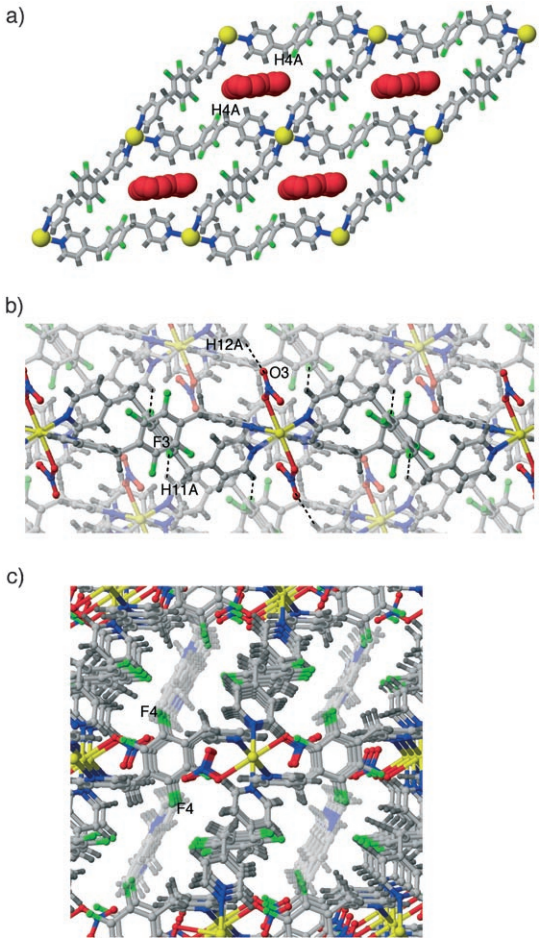

Figure 2. Crystal structure of **2a**: a) top view of the 2D sheet; b) side view of the stacking sheets; c) top view of the stacking sheets.

$(NO_3)_2$, two bpf molecules, and an *o*-bromoanisole molecule. The sheet structure of **2c** is shown in Figure S2a (see Supporting Information). In contrast to **2a**, whose *N*,*N*-dimethylaniline guest molecules are present in a disordered pattern, the *o*-bromoanisole molecules in **2c** are clathrated alternately in each cavity.

{[Cd(bpf)$_2$(NO$_3$)$_2$]·naphthalene}$_n$ (2d): The structure of **2d** is also analogous to **2c** except that the unit cell consists of one and a half equivalents of $Cd(NO_3)_2$, two bpf molecules, and a naphthalene molecule and the corresponding dimension of the *c* axis is 31.774(5) Å. The sheet structure of **2d** is shown in Figure S2b (see Supporting Information). There are two types of cavities with slightly different sizes which are alternately linked to each other. The naphthalene molecules are also clathrated in each cavity.

{[Cd(bpf)$_2$(NO$_3$)$_2$]·(*p*-C$_6$H$_4$BrMe)$_2$}$_n$ (3): The sheet structure of **3** is shown in Figure 3a. It contains four crystallographically independent *p*-bromotoluene molecules whose bromine atom and methyl group are disordered. There are two types of cavities with alternate linking of alignments, each of which contains three *p*-bromotoluene molecules. Cavities A and B have diagonal-to-diagonal distances of 29.48×14.93 and 28.44×16.34 Å and dimensions of 16.56×16.48 and 16.56×16.34 Å, respectively. The 2D sheet is relatively flat,

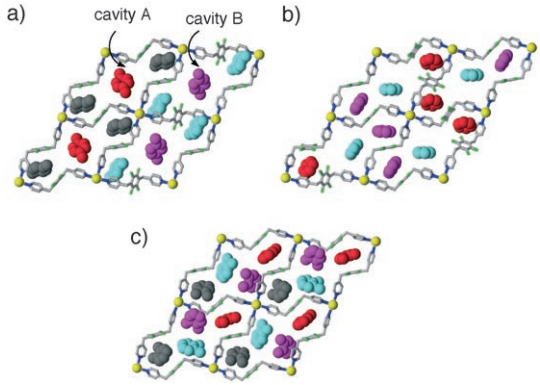

Figure 3. Top views of the 2D sheet structures of a) **3**, b) **4**, and c) **5a**. Hydrogen atoms and nitrate anions have been omitted for clarity. The crystallographically independent guest molecules are represented in different colors and by a space filling model.

and is made up into layers stacked and eclipsed on each other along the *a* axis, with an interplanar distance of 5.6 Å (see Figure S3 in the Supporting Information). It is clear that two guest molecules on each side of the cavity are clathrated across adjacent sheets.

$\{[Cd(bpf)_2(NO_3)_2]\cdot(C_6H_6)_3\}_n$ (4): The sheet structure of **4** is shown in Figure 3b. The diagonal-to-diagonal distances are 29.28×15.03 Å and the dimensions of the grid are 16.69×16.69×16.52×15.95 Å. Three benzene molecules are clathrated in each cavity. This sheet is made up into layers stacked and eclipsed on each other along the *c* axis. The interplanar distance is 5.8 Å.

$\{[Cd(bpf)_2(NO_3)_2]\cdot(o\text{-}C_6H_4Me_2)_4\}_n$ (5a): The sheet structure of **5a** is shown in Figure 3c as a typical example. The diagonal-to-diagonal distances are 29.43×16.24 Å and the dimensions of the grid are 16.97×16.97×16.69×16.69 Å. Four *o*-xylene molecules are clathrated in each cavity. One of the guest molecules is clathrated between two tetrafluorophenylene rings with separations of 3.7 and 4.2 Å, while one of the other guest molecules is clathrated through the pyridine ring with a separation of 3.6 Å. The enclathration ability of the *o*-xylene network **5a** appears to be different to that of the benzene network **4**, in which three guest molecules are accommodated, because the benzene molecule is significantly smaller than *o*-xylene. Two of the four guest molecules in the cavity of **5a** are, in fact, clathrated across adjacent sheets (pink and light blue molecules in Figure 3c). A side view of the stacking of **5a** is shown in Figure S4a (see Supporting Information). Interestingly, the adjacent sheets are enantiomers of each other and are stacked alternately. The same enantiomers are eclipsed whereas the opposite enantiomers are staggered with an interplanar distance of 6.4 Å.

$\{[Cd(bpf)_2(NO_3)_2]\cdot(PhOCOMe)_2\}_n$ (6a): In addition to the 1D chain and 2D sheet structures, 3D networks with a diamond topology are also formed from $Cd(NO_3)_2$ and bpf with only very small changes in guest structures. The 3D diamond network in **6a–h** seems to be the most stable structure for Cd/bpf networks as most varieties of guest organic molecule afford this structure. The coordination environment at Cd^{II} is the same as those of the other bpf complexes. The crystal structure of **6a** belongs to space group *C*2/*c* and contains half a molecule of $Cd(NO_3)_2$, one bpf molecule, and one phenyl acetate molecule per unit cell. All the ligands adopt *trans* conformations. The resulting extended structure is a 3D diamond framework. The diamond net can be broken down into an adamantane skeleton that consists of four six-membered windows. The adamantane skeleton structure of **6a** is shown in Figure 4a. The distances between adjacent Cd^{II} ions are 16.62 and 16.60 Å, while the Cd-Cd-Cd angles range from 58.26 to 148.73°, thereby creating large cavities. This shows that the diamond framework is considerably deformed due to the flexibility of the ligand. The phenyl acetate molecules are clathrated near the pyridine rings in the large adamantane unit through a C–H···F hydrogen bond with an H23A···F4 distance of 2.509 Å. The bulk of the void space is filled by threefold interpenetration of the identical frameworks (Figure 4b) linked by two types of hydrogen bonds. The N3–O3···H6B, H10A···F1,

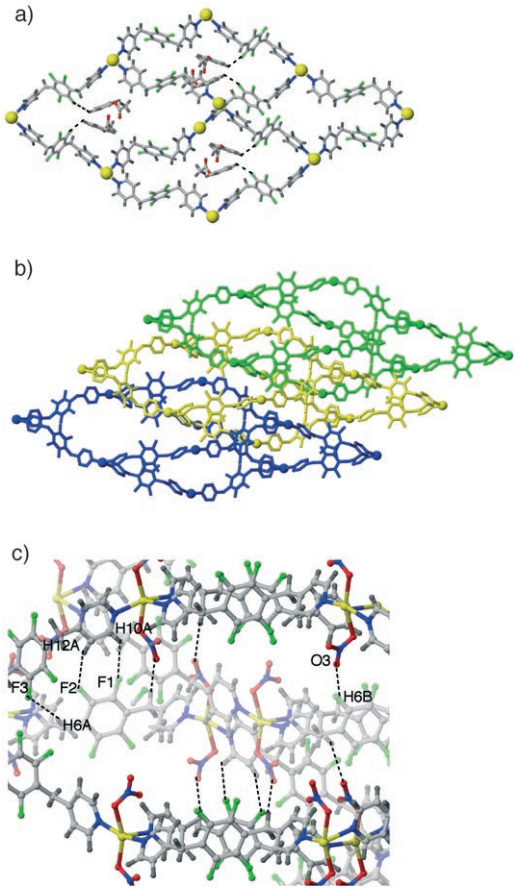

Figure 4. Crystal structure of **6a**: a) view of the 3D adamantane skeleton with guest molecules linked by hydrogen bonds; b) view of the threefold interpenetrating networks; c) hydrogen bonds between the interpenetrating networks.

H12A···F2, and H6A···F3 distances are 2.318, 2.531, 2.539, and 2.401 Å (Figure 4c). It is noteworthy that all the fluorine atoms participate in hydrogen bonds.

$\{[Cd(bpfb)_2(NO_3)_2]\cdot(EtOH)_2\}_n$ (7): The reaction of $Cd(NO_3)_2$ with bpfb in the absence of aromatic compounds afforded the simple 2D rhombus grid network **7**, as shown in Figure 5. The diagonal-to-diagonal distances are 35.20×

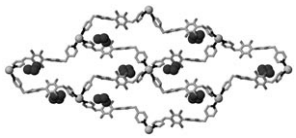

Figure 5. Top view of the 2D sheet structure of **7**. Hydrogen atoms and nitrate anions have been omitted for clarity. The guest molecules are represented by a space filling model. One of the guest molecules is disordered.

15.05 Å and the dimensions of the grid are 19.28×19.28×19.00×19.00 Å. Two molecules of EtOH are clathrated in each cavity. Because the fluorine atoms of the ligands tend toward the inner cavity, the grid structure is considerably distorted to fit around guest molecules that are smaller than aromatic compounds.

$\{[Cd(bpfb)_2(NO_3)_2]\cdot(PhOCOMe)_2\}_n$ (8a): The reaction of bpfb with $Cd(NO_3)_2$ in the presence of aromatic compounds such as phenyl acetate, *N*,*N*-dimethylaniline, or *m*-dimethoxybenzene afforded interpenetrating 2D rhombus grid sheets with an $ML_2\cdot G_2$ composition. The sheet structure of **8a**, which contains phenyl acetate molecules as guests, is shown in Figure 6a. The crystal structure belongs to space group *Pccn* and all the ligands adopt *trans* conformations. Each cavity surrounded by four Cd^{II} atoms and four bpfb ligands contains two molecules of phenyl acetate as guests. The diagonal-to-diagonal distances and the dimensions of the 2D rhombus grid are 34.10×16.45 Å and 18.93 Å, respectively. Each guest molecule is packed between the perfluoroaromatic rings of the host framework with face-to-face interactions. The shortest intermolecular contact (C16···C27) is 3.245 Å, with an interplanar angle of about 11°. The guest aromatic rings are also linked to the opposite perfluoroaromatic ring through C–H···F hydrogen bonds (H26A···F3 2.572 Å). The large cavity is filled by twofold parallel interpenetration of the identical frameworks. The puckered sheet of **8a** is shown in Figures 6b and 6c; two sheets engage complementarily in parallel interpenetration to form a planar layer. The mode of interpenetration is topologically identical to the recently reported interpenetrating coordination network structures of $[Co(Py_2S)_2Cl_2]_n$,[14] $[Cd_2(NO_3)_4(Py_2C_3H_6)_4(H_2O)]_n$,[15] $[Mn_2(NCS)_4(Py_2C_3H_6)_4]_n$,[16] and $[Fe(N_3)_2(Py_2C_3H_6)_2]_n$.[17] The interpenetrating cyclic framework is shown in Figure 6d. Each framework is linked by two types of hydrogen bonds. The N3–O2···H19B and H11A···F3 distances are 2.539 and 2.635 Å, respectively. Interestingly, the adjacent layers are eclipsed by a 180° rotation around the vertical *c* axis of the layers. These layers are stacked in a staggered manner and alternate layers are eclipsed completely, with an interplanar distance of 10.5 Å (Figure 6e). Each layer is linked by C–H···F hydrogen bonds, as shown in Figure 6f. The H6A···F7 and H6B···F7 distances are 2.647 and 2.719 Å, respectively. The structures of **8b** and **8c** are identical to that of **8a** and have the same space group (*Pccn*).

$\{[Cd(bpfb)_2(NO_3)_2]\cdot(biphenyl)_2\}_n$ (8d): Although the host framework of **8d** is a rhombus-based 2D grid with twofold

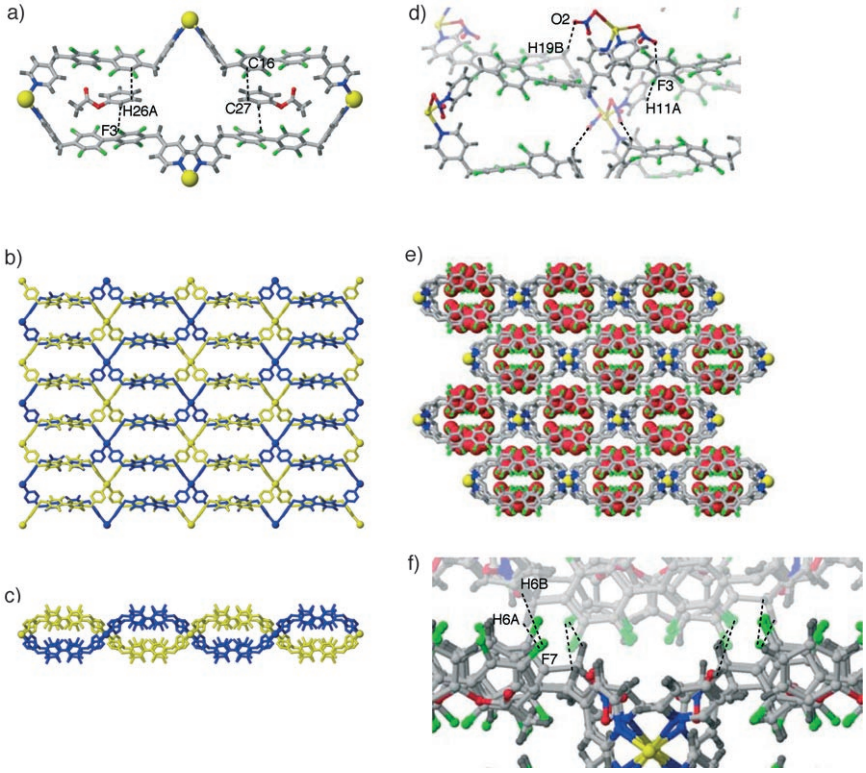

Figure 6. Crystal structure of **8a**: a) top view of the cyclic cavity with guest molecules linked by hydrogen bonds; b) top view of the twofold parallel interpenetration of 2D rhombic grids along the *b* axis; c) side view of the twofold parallel interpenetration of 2D rhombic grids along the *c* axis; d) hydrogen bonds between the interpenetrating networks; e) side view of the stacking layers along the *c* axis; f) side view of the stacking layers linked by hydrogen bonds.

parallel interpenetrating networks, similar to **8a–c**, the packing mode is different. The two benzene rings of the guest biphenyl molecule are in simultaneous contact with two tetrafluoroaromatic rings of the ligand. The shortest intermolecular contacts (C16···C29 and C9···C35) are 3.545 and 3.583 Å, respectively. The guest aromatic rings are also linked to the opposite perfluoroaromatic ring by C–H···F hydrogen bonds (H29A···F1 2.734, H30A···F3 2.773 Å). The layers slide to align Cd^{II} ions along the *a* axis, which results in a lengthening of the interplanar distance from 10.5 to 12.5 Å (Figure 7b) and a different space group (*Pcca*). These layers are actually staggered, as can be seen in the side view down the *b* axis, and alternate layers are completely eclipsed. Solvent molecules of EtOH and H_2O fill the vacancies between the layers. Nevertheless, channels are still observed in the solid along the *a* axis (see Figure S5 in the Supporting Information).

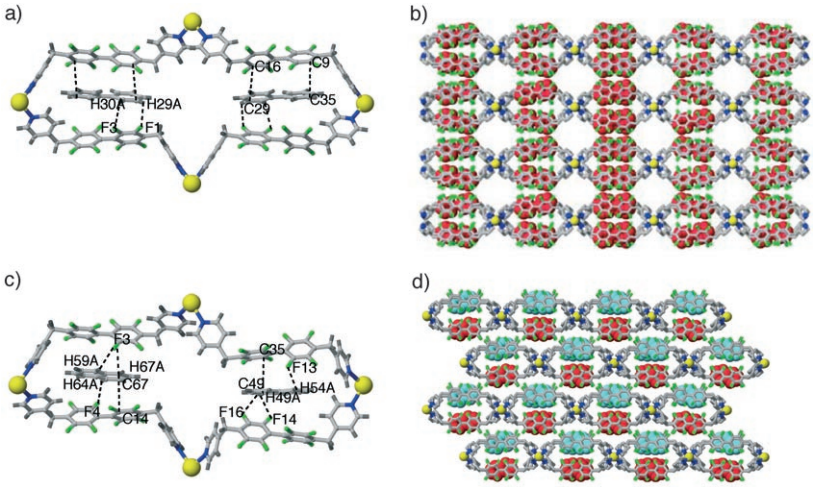

Figure 7. Views of the interpenetrating 2D layers of **8d** and **8e**. a) top view of the cyclic cavity of **8d** linking guest molecules by hydrogen bonds; b) side view of stacking layers of **8d**; c) top view of the cyclic cavity of **8e** linking guest molecules by hydrogen bonds; d) side view of stacking layers of **8e**. Two crystallographically independent molecules of naphthalene are represented in different colors (red and light blue).

$\{[Cd(bpfb)_2(NO_3)_2]\cdot(naphthalene)_2\}_n$ (8e): Remarkably, formation of an asymmetrical alignment of layers occurs in **8e** (space group *Cc*). The host framework is analogous to those of **8a–d**, as shown in Figure S6a (see Supporting Information). The diagonal-to-diagonal distances are 33.75 × 16.96 Å and the dimensions of the grid are 18.96 × 18.96 × 18.81 × 18.81 Å. Both of the guest naphthalene molecules, which are crystallographically independent, are in contact with two perfluoroaromatic rings of alternate ligands. However, the face-to-face interactions are weaker than those in **8a** and **8d**. The shortest intermolecular contacts (C14···C67 and C35···C49) are 3.881 and 3.771 Å, respectively. The guest aromatic rings are linked with perfluoroaromatic ring by C–H···F hydrogen bonds (H59A···F3 2.616, H67A···F3 2.754, H64A···F4 2.531, H54A···F13 2.647, H49A···F14 2.744, and H49A···F16 2.784 Å). The packing mode of the layers is shown in Figure 7d. All the layers are stacked in an eclipsed manner with an interplanar distance of 10.6 Å. In consequence, channels run in the solid between the *a* and *b* axes (see Figure S6b in the Supporting Information).

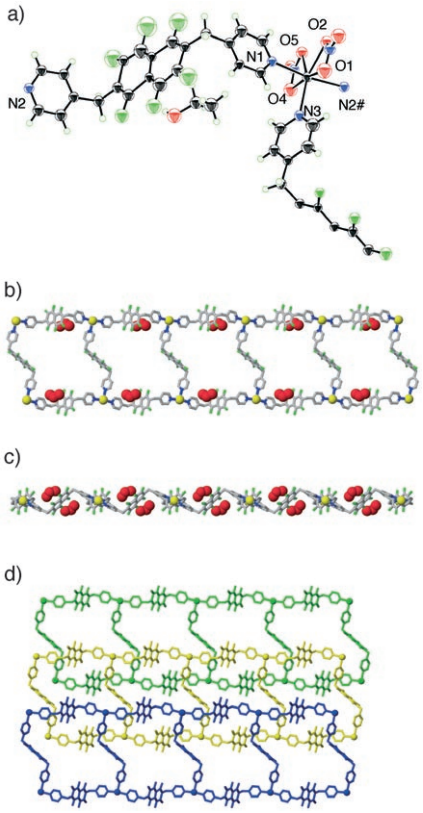

Figure 8. Crystal structure of **9**: a) ORTEP view around the metal center. Thermal ellipsoids are shown with 50% probability; b) top view of the 1D ladder; c) side view of the 1D ladder; d) stacking of 1D ladders. Hydrogen atoms and nitrate anions have been omitted for clarity.

$\{[Cd(2,6\text{-bpfn})_{1.5}(NO_3)_2]\cdot EtOH\}_n$ (9): The reaction of 2,6-bpfn with $Cd(NO_3)_2$ in the absence of aromatic compounds afforded the 1D ladder network **9**. Solvent EtOH molecules are clathrated in the coordination ladder. The coordination geometry is heptacoordinate, as shown in Figure 8a. Three ligand pyridyl moieties, all of which adopt *trans* conformations, form a T-shaped arrangement at the metal ion, and the remaining coordination sites are occupied by two bidentate nitrate anions. The T-shaped connecting units are linked to give a 1D ladder framework, as shown in Figure 8b. Each

cavity surrounded by four Cd^{II} atoms and four ligands clathrates two EtOH molecules. The diagonal-to-diagonal distance and the dimensions of the ladder are 27.12×23.67 and 17.52×18.46 Å, respectively. The side view of the ladders is shown in Figure 8c. These zigzag 1D ladder frameworks align parallel to each other to fill the bulk of the void space in each cavity (Figure 8d).

{[Cd(2,6-bpfn)$_2$(NO$_3$)$_2$]·(*p*-C$_6$H$_4$(OMe)$_2$)$_2$}$_n$ (10a): A top view of the 2D rhombus grid sheet of **10a** is shown in Figure 9a. The crystal structure belongs to the space group *C*2/*c*, and all the ligands adopt *trans* conformations. Each cavity clathrates two *p*-dimethoxybenzene molecules as guests. The distances between diagonal Cd^{II} ions are 33.63×13.60 Å, and the grid dimensions are 18.14 Å. There are effective face-to-face interactions between the perfluoroaromatic ring of the host and the aromatic ring of guest in which the shortest intermolecular contract (C10···C28) is 3.411 Å. A side view of the sheets' stacking is shown in Figure 9b. Interestingly, adjacent sheets are enantiomers of each other, with alternate stacking: the homochiral species are eclipsed whereas the heterochiral species are staggered, with an interplanar distance of 6.3 Å. Each layer is linked by two types of hydrogen bonds, as shown in Figure 9c. The N3–O3···H20A and H4A···F3 distances are 2.525 and 2.520 Å, respectively. Moreover, the guest aromatic rings are linked by C–H···F hydrogen bonds with neighboring sheets (H27A···F2 2.653 Å).

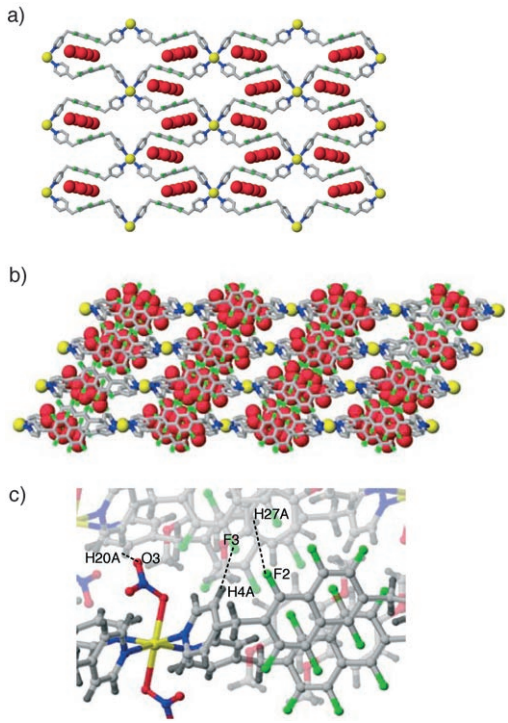

Figure 9. Crystal structure of **10a**: a) top view of the 2D sheet between the *a* and *c* axws; b) side view of stacking 2D sheets along the *b* axis; c) side view of the stacking sheets linked by hydrogen bonds.

The structure of **10b** is identical to that of **10a** and has the same space group (*C*2/*c*).

{[Cd(2,6-bpfn)$_2$(NO$_3$)$_2$]·(biphenyl)$_2$}$_n$ (10c): The sheet structure of **10c** is shown in Figure 10. There are two cavities with alternate linking of alignments; these cavities are exactly rhomboid. The diagonal-to-diagonal distances are 35.34×15.36 and 33.71×16.03 Å and the dimensions of the grid are 18.83×19.69 and 18.83×18.49 Å in cavities A and B, respectively. Although three biphenyl molecules are apparently enclosed in each cavity, these are disordered and/or are clathrated across the sheets. As a consequence, the grid framework is capable of swelling (cf. the shorter diagonals of **10a**). These layers are stacked on each other in an eclipsed manner, with an interplanar distance of 6.4 Å (see Figure S7 in the Supporting Information).

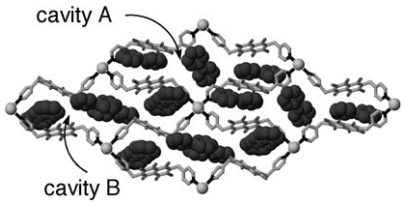

Figure 10. Top view of the 2D sheet of **10c**. Hydrogen atoms and nitrate anions have been omitted for clarity. The guest molecules are represented by a space filling model.

{[Cd(2,6-bpfn)$_2$(NO$_3$)$_2$]·(*p*-C$_6$H$_4$Me$_2$)$_2$}$_n$ (11a): The most common framework with 2,6-bpfn is a twisted 2D grid-type sheet with an $ML_2{\cdot}G_2$ stoichiometry. A top view of the sheet structure is shown in Figure 11a. The coordination environment of Cd^{II} in **11a** is similar to those in **10a–c**. All the ligands adopt *cis* conformations, unlike the 2D grid sheet structures of **10a–c**, in which all ligands adopt *trans* conformations. The topology of this sheet is the same as the grid structures with a [4,4] topology; each cavity is surrounded by four Cd^{II} ions and four ligands. Two types of cavities are alternately repeated, and each encloses two *p*-xylene molecules. The larger cavity (cavity A) can enclose two *p*-xylene molecules edge-to-edge. In the smaller cavity (cavity B), the host framework ring is extremely twisted and each half-isolated void is filled with a *p*-xylene molecule. Efficient face-to-face interactions between the perfluoroaromatic rings of the host framework and the guest molecules are observed. Two guest molecules in the twisted smaller cavity B are clathrated between two perfluoroaromatic rings, with a shortest intermolecular contact (C15···C29) of 3.762 Å, while two guest molecules in the larger cavity A are clathrated between two perfluoroaromatic rings of adjacent layers with a shortest intermolecular contact (C10···C25) of 3.353 Å (Figure 11c). The layer is flat and thick, which results in large channels between the *a* and *b* axes in which the guest mole-

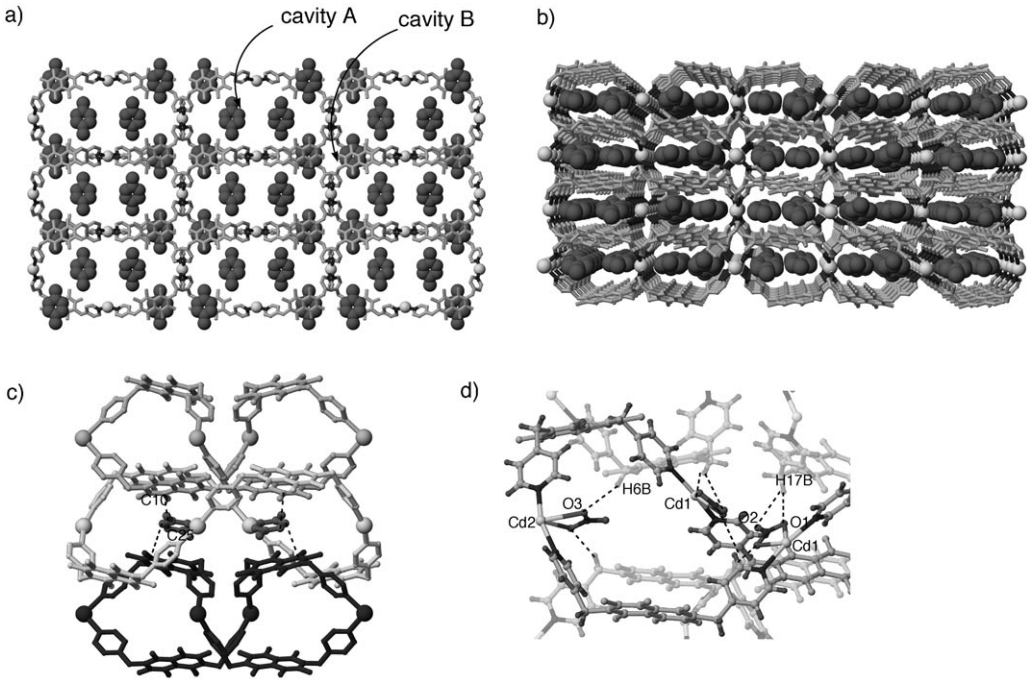

Figure 11. Crystal structure of **11a**: a) top view of the 2D sheet along the *b* axis; b) view of channels along the *a* axis; c) view of the clathrated guest molecule between adjacent layers in larger cavity A; d) hydrogen bonds between the adjacent sheets.

cules are clathrated in parallel fashion. A side view of the sheets' stacking is shown in Figure 11b. The adjacent sheets, which are enantiomers of each other, are stacked alternately and staggered, with an interplanar distance of 7.8 Å. Each sheet is linked by hydrogen bonds, as shown in Figure 11d. The N1−O1···H17B, N1−O2···H17B, and N2−O3···H6B distances are 2.399, 2.699, and 2.660 Å, respectively.

{[Cd_2(2,6-bpfn)$_3$(NO_3)$_4$]·PhNHMe}$_n$ (12): The coordination geometry around the Cd^{II} ion in **12** is heptacoordinate, as for **9**. Figure 12a shows a herringbone sheet with disordered guest molecules. Each cavity is surrounded by six Cd^{II} ions and six ligands and can apparently clathrate three guest molecules. The large cavities are filled by two adjacent sheets and the guest molecule is clathrated between the fluorinated naphthalene rings of ligands from different frameworks, with effective face-to-face interactions (Figure 12b). One guest molecule is clathrated in the center of a large cavity in a herringbone topology. Each guest molecule is clathrated between two perfluoroaromatic rings of adjacent layers, with a shortest intermolecular contact (C8···C38) of 3.407 Å. This puckered sheet is made up into layers stacked on top of each other, with an interplanar distance of 2.9 Å. As a consequence, the sequence of the three herringbone sheets is of the ABC type with an M_2L_3·G composition. Channels run along the *a* axis, as shown in Figure S8 (see Supporting Information).

{[Cd(2,7-bpfn)$_2$(NO_3)$_2$]·(*m*-C_6H_4(OMe)$_2$)$_2$}$_n$ (13): A top view of **13**, whose structure is identical to those of 2,6-bpfn networks **10a** and **10b**, with the same space group (*C*2/*c*), is

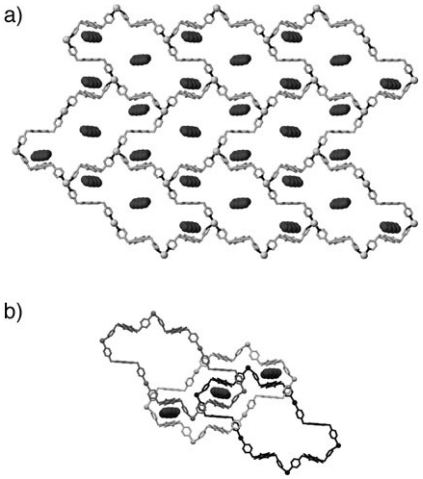

Figure 12. Views of the herringbone sheet structure of **12**: a) top view of the 2D sheet along the *a* axis; b) top view of the clathrated guest molecule between two adjacent sheets. Hydrogen atoms and nitrate anions have been omitted for clarity.

shown in Figure 13. The distances between diagonal Cd^{II} ions are 32.29×13.53 Å, and the dimension of the grid is 17.51 Å. Two *m*-dimethoxylbenzene molecules are clathrated in each cavity, in which there are effective face-to-face interactions and a shortest intermolecular contact (C10···C27) of 3.300 Å. A side view of the stacking is shown in Figure S9a (see Supporting Information). The sheet is relatively flat and thick, and is made up into layers stacked on each other with an interplanar distance of 7.2 Å. Each sheet is linked by two types of hydrogen bonds. The N3−

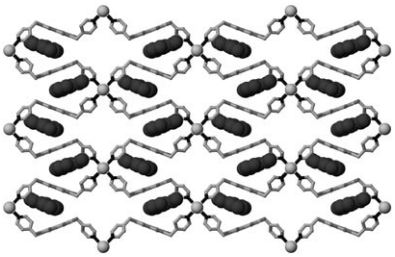

Figure 13. Top view of the 2D sheet of **13**. Hydrogen atoms, nitrate anions, and clathrated solvent molecules have been omitted for clarity.

O3···H17B, H2A···F1, and H4A···F5 distances are 2.414, 2.514, and 2.654 Å, respectively.

{[Cd(2,7-bpfn)$_2$(NO$_3$)$_2$]·(*m*-C$_6$H$_4$Me$_2$)$_2$}$_n$ (14a): The propagation of the 2D sheet structure in this complex is shown in Figure 14a. The coordination geometry around the Cd^{II} ion is similar to that of **13**, except for the *cis* conformation of the 2,7-bpfn ligand. Although the topology is same as that of a grid, the appearance of the sheet is far from it. Each cavity is shaped like a dumbbell, and two *m*-xylene molecules are clathrated in both "weights" of the dumbbell by face-to-face interaction with the perfluoroaromatic rings of the host, with a shortest C···C intermolecular contact (C11···C24) of 3.620 Å. A side view of the stacking is shown in Figure 14b. The parallel infinite layers of the puckered sheets are eclipsed, with a separation of 8.0 Å. Each layer is linked by hydrogen bonds, as shown in Figure 14c. The N3–O2···H9 and N3–O2···H11 distances are 2.524 and 2.614 Å, respectively. Channels with dumbbell shapes run perpendicularly to the planes along the grid sheets (Figure 14d).

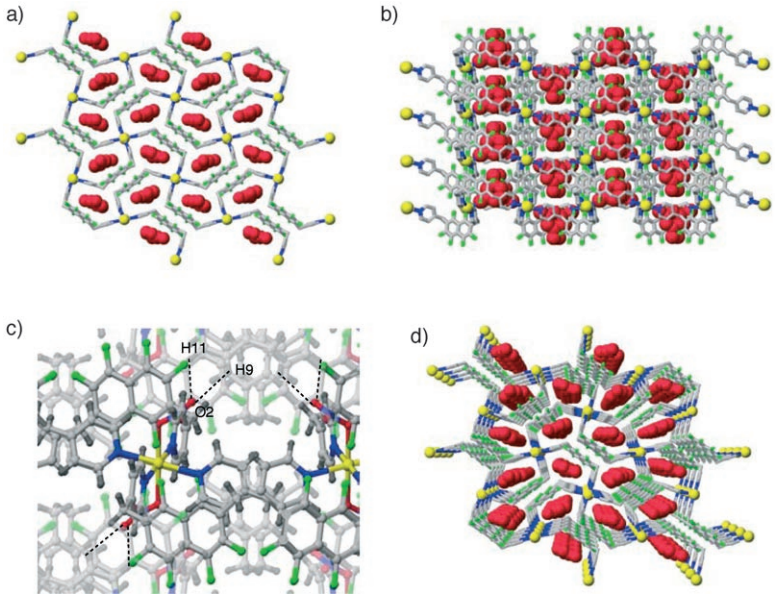

Figure 14. Crystal structure of **14a**: a) top view of the 2D sheet along the *a* axis; b) side view of the stacking 2D sheets along the *c* axis; c) side view of the stacking sheets linked by hydrogen bonds; d) view of channels along the *a* axis. Hydrogen atoms and nitrate anions have been omitted for clarity.

The influence of fluorine atoms: The remarkable enclathration ability of these coordination networks is caused by the fluorine atoms contained in the flexible ligands. The importance of the perfluoroaromatic rings was demonstrated by controlled experiments with the nonfluorinated ligand 1,4-bis(4-pyridylmethyl)benzene (bpb), which is an analogue of bpf. We attempted to obtain clathrate networks from Cd(NO$_3$)$_2$ and bpb in the presence of a large excess of *N*,*N*-dimethylaniline, *m*-xylene, or phenyl acetate under the same reaction conditions as for bpf. All the attempts were unsuccessful and we obtained an interpenetrating infinite ladder structure that has been reported previously.[13,18]

The fluorine atoms of the ligands are mainly responsible for their high enclathration ability. Ever since a stable 1:1 complex of benzene and perfluorobenzene consisting of a face-to-face stack of alternating molecules was reported in 1960,[19] arene–perfluoroarene interactions have been utilized as organizational motifs in crystal engineering.[20] In addition to the face-to-face interactions, C–H···F interactions have been discussed in the crystal structures of hydroaromatic and perfluoroaromatic molecules with a H···F separation of around 2.3–2.7 Å.[20e,21] Most flexible coordination networks have effective C–H···F interactions between the host perfluoroaromatic frameworks and guest aromatic rings, as well as between the individual host networks through the methylene or pyridine H atoms. Interestingly, bpfb, 2,6-bpfn, and 2,7-bpfn networks have more efficient face-to-face interactions than bpf networks because of their larger perfluoroaromatic rings, with the shortest C···C contact ranging from around 3.2 to 3.8 Å.

The flexibility of the ligands is affected by the guest molecules: The flexibility of the bridging ligands is very important for constructing clathrate coordination networks that vary in the size, shape, and number of guest organic molecules. In the case of bpf networks, guest aromatic compounds containing bulky groups, such as *tert*-butylbenzene, are suitable for a 1D chain structure with a cyclic cavity in which all the ligands adopt *cis* conformations, whereas planar guest molecules such as *N*,*N*-dimethylaniline prefer a 2D grid sheet in which all the ligands adopt *trans* conformations. The presence of methylene groups between the pyridine and tetrafluorophenylene moieties causes a dependence of the network structure on the guest molecules. A typical example of the *cis*–*trans* conversion can be seen for **13**, **14a**, and **14b**, which have the same

2,7-bpfn ligand. All the ligands in **13** (rhombus 2D grid framework) adopt a *trans* conformation, while in **14a**,**b** (2D grid with dumbbell-shaped cavity) they adopt a *cis* conformation, with the same topology of the rhombus grid.

Interestingly, 2D grid networks with bpf can be elastic depending on the number of guest molecules. A comparison of the structures of **2a**, **3**, **4**, and **5a** shows that the size of each cavity becomes larger as the number of guest molecules per cavity increases, as shown in Figure 15. Note that three

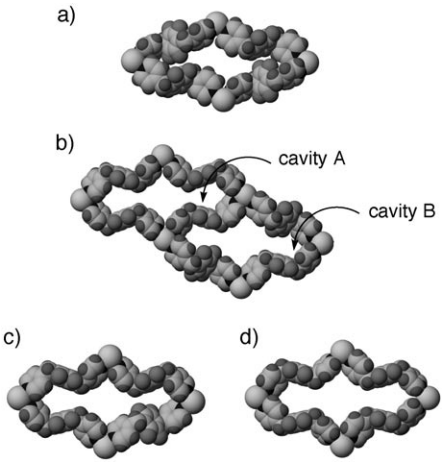

Figure 15. Space-filling views of a cavity of **2a** (a), **3** (b), **4**, (c), and **5a** (d). Nitrate anions and guest molecules have been omitted for clarity.

guest molecules per cavity are considered for **3**. The bulk of the void space increases gradually with the number of guest molecules due to structural variation of the coordination framework. Focusing on the arrangement of pyridine and tetrafluorophenylene in **2a**, the edges of two opposing pyridine rings point towards the inside of the cavity, and two neighboring tetrafluorophenylene groups are in contact through edge-to-face interactions, with a shortest C···F distance of 3.63 Å. Consequently, the cavity has no space around the metal cations and is filled with only one guest molecule at the center of the cavity. In contrast, the cavities of **3**, **4**, and **5a** have enough space for three or four guest molecules because the planes of the tetrafluorophenylene groups tend to face towards the inside of the cavity. These differences are attributed to the conformational freedom around the methylene group between the pyridine and tetrafluorophenylene rings. Figure 16 shows Newman projections of the ligands contained in **2a** and **5a**. The dihedral angles in **2a** are 92.43° and 112.19°, and those in **5a** range from 91.06° to 101.76°. A high value for this angle means that the tetrafluorophenylene ring occupies a space in the cavity, whereas a value near to 90° results in a void space in the cavity. The metal–metal distances in a cavity can also vary accordingly. The shorter diagonal–diagonal distances increase from 13.11 to 16.24 Å as the number of guest molecules increases (the mean distance in **3** is 15.73 Å, which is

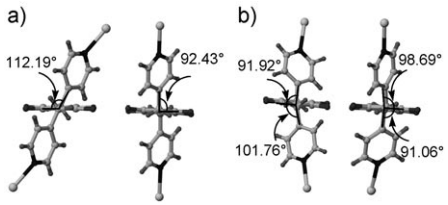

Figure 16. Views of the conformations around the methylene groups of **2a** (a) and **5a** (b).

between those of **4** and **5a**). These values are consistent with their enclathration abilities.

Conclusion

We have demonstrated that the fluorinated flexible ligands bpf, bpfb, 2,6-bpfn, and 2,7-bpfn form a variety of clathrate coordination networks with Cd^{II} in the presence of organic molecules. The diversity of network topologies is induced by interactions between the guest molecules and the flexible ligand frameworks. While host networks are mainly retained by O···H hydrogen bonds with the nitrate anions, guest organic molecules are mainly retained by the host networks by forming intermolecular interactions with the perfluoroaromatic rings. Host–guest C–H···F hydrogen bonds are formed for all the networks, whereas efficient face-to-face interactions between hydroaromatic and perfluoroaromatic rings are formed predominantly in the bpfb, 2,6-bpfn, and 2,7-bpfn systems. We have therefore developed a series of guest-dependent flexible coordination networks that open the way to new possibilities for metal–ligand architectures with novel structures and topologies.

Experimental Section

Synthesis

Materials and instruments: All reactions involving organometallic compounds were carried out under nitrogen. THF was dried with sodium and distilled. *n*-Butyllithium (hexane solution) was purchased from Kanto Chemical Co. Ltd. Perfluoroaromatic compounds were purchased from Tokyo Chemical Industry Co., Ltd. Diisopropylamine and 4-picoline were dried over potassium hydroxide and distilled. Coordination networks were prepared in air. $Cd(NO_3)_2{\cdot}4H_2O$ was purchased from Nacalai Tesque Co. Ltd. Guest compounds such as *tert*-butylbenzene or *N*-methylaniline were purchased from Tokyo Chemical Industry Co. Ltd. or Kanto Chemical Co. Ltd. ^1H and ^{13}C NMR spectra of ligand products in $CDCl_3$ (containing 1% TMS) were recorded with a JEOL EX-400 FT NMR spectrometer at 25 °C.

1,4-Bis(4-pyridylmethyl)tetrafluorobenzene (bpf): Butyllithium (1.6 M hexane solution, 30 mmol) was added to a solution of diisopropylamine (4.2 mL, 30 mmol) in THF (20 mL) at 0 °C. Stirring for 30 min at the same temperature gave lithium diisopropylamide (LDA) in situ, which was added to a solution of 4-picoline (1.5 mL, 15 mmol) in THF (30 mL) at −78 °C. After stirring for 5 min, the reaction mixture was allowed to warm up to room temperature and stirred for a further 1 h. Perfluorobenzene (0.58 mL, 5 mmol) in THF (30 mL) was then added to the reaction mixture at −78 °C. After stirring for 5 min, the reaction mixture was al-

lowed to warm up to room temperature and stirred for a further 24 h. After quenching with distilled water, the organic compounds were extracted with chloroform. The organic layer was washed with saturated NaCl and dried with $MgSO_4$. Filtration followed by concentration provided a solid. After column chromatography (silica gel, ethyl acetate), the desired compound bpf was obtained as a pure product in 90% yield (3.0 g). ^{1}H NMR ($CDCl_3$, TMS): $\delta = 4.04$ (s, 4H), 7.16 (pseudo d, $J = 5.9$ Hz, 4H), 8.52 ppm (pseudo d, $J = 6.0$ Hz, 4H); ^{13}C NMR ($CDCl_3$, TMS): $\delta = 28.02$, 116.57, 123.62, 144.75 (dm, $J_{C,F} = 232.7$ Hz), 146.32, 150.22 ppm; HRMS calcd for $C_{18}H_{12}F_4N_2$: 332.09358; found 332.09495.

4,4′-Bis(4-pyridylmethyl)octafluorobiphenyl (bpfb): This compound was prepared from decafluorobiphenyl (0.33 g, 1 mmol) in a similar manner as described above in 68% yield (0.33 g). ^{1}H NMR ($CDCl_3$, TMS): $\delta = 4.14$ (s, 4H), 7.24 (pseudo d, $J = 5.4$ Hz, 4H), 8.58 ppm (pseudo d, $J = 6.4$ Hz, 4H); ^{13}C NMR ($CDCl_3$, TMS): $\delta = 28.29$, 105.96, 119.82, 123.73, 144.05 (dm, $J_{C,F} = 253.7$ Hz), 144.43 (dm, $J_{C,F} = 242.6$ Hz), 145.78, 150.35 ppm; HRMS calcd for $C_{24}H_{12}F_8N_2$: 480.08718; found 480.08796.

2,6-Bis(4-pyridylmethyl)hexafluoronaphthalene (2,6-bpfn): The title compound was prepared from octafluoronaphthalene (2.72 g, 10 mmol) in a similar manner as described above in 27% yield (1.13 g). ^{1}H NMR ($CDCl_3$, TMS): $\delta = 4.19$ (s, 4H), 7.20 (pseudo d, $J = 5.9$ Hz, 4H), 8.53 ppm (pseudo d, $J = 6.4$ Hz, 4H); ^{13}C NMR ($CDCl_3$, TMS): $\delta = 28.20$, 111.30, 116.79, 123.65, 140.62 (dm, $J_{C,F} = 251.0$ Hz), 145.78 (dm, $J_{C,F} = 244.5$ Hz), 146.27, 150.25, 150.25 ppm (dm, $J_{C,F} = 253.7$ Hz); HRMS calcd for $C_{22}H_{12}F_6N_2$: 418.09038; found 418.09052.

2,7-Bis(4-pyridylmethyl)hexafluoronaphthalene (2,7-bpfn): The title compound was prepared from octafluoronaphthalene (2.72 g, 10 mmol) in a similar manner as described above in 25% yield (1.07 g). ^{1}H NMR ($CDCl_3$, TMS): $\delta = 4.04$ (s, 4H), 7.16 (pseudo d, $J = 5.9$ Hz, 4H), 8.52 ppm (pseudo d, $J = 6.0$ Hz, 4H); ^{13}C NMR ($CDCl_3$, TMS): $\delta = 28.02$, 115.47, 123.62, 140.68 (dm, $J_{C,F} = 275.8$ Hz), 146.32, 146.59 (dm, $J_{C,F} = 248.3$ Hz), 150.22, 150.32 (dm, $J_{C,F} = 262.8$ Hz) ppm; HRMS calcd for $C_{22}H_{12}F_6N_2$: 418.09038; found 418.0885.

General procedure for the synthesis of coordination networks: A solution of bpf (20 mg, 0.06 mmol) in ethanol (1 mL) was added to a solution of $Cd(NO_3)_2{\cdot}4H_2O$ (9.3 mg, 0.03 mmol) in H_2O (0.25 mL). After stirring for 1 min and filtration, the guest compound (1.9 mmol) was added slowly. The mixture was then allowed to stand for 48 h at room temperature to give crystals.

$\{[Cd(bpf)_2(NO_3)_2]\cdot PhtBu\}_n$ (1a): The general procedure described above was followed with *tert*-butylbenzene (0.29 mL, 1.9 mmol) to give the title compound as colorless, plate-shaped crystals in 53% yield (17 mg). Elemental analysis calcd (%) for $C_{47}H_{42}CdF_8N_6O_7$ ($[Cd(bpf)_2(NO_3)_2]\cdot$*tert*-butylbenzene$\cdot(EtOH)_{0.5}\cdot(H_2O)_{0.5}$): C 52.89, H 3.97, N 7.87; found: C 52.51, H 4.08, N 7.58.

$\{[Cd(bpf)_2(NO_3)_2]\cdot PhCHMe_2\}_n$ (1b): The general procedure described above was followed with $Cd(NO_3)_2{\cdot}4H_2O$ (19 mg, 0.06 mmol) in H_2O (0.5 mL), bpf (40 mg, 0.12 mmol) in ethanol (2 mL), and cumene (0.53 mL, 3.8 mmol). The title compound was obtained as colorless, plate-shaped crystals in 58% yield (37 mg). Elemental analysis calcd (%) for $C_{46}H_{40}F_8CdN_6O_7$ ($[Cd(bpf)_2(NO_3)_2]\cdot PhCHMe_2\cdot(EtOH)_{0.5}\cdot(H_2O)_{0.5}$): C 52.46, H 3.83, N 7.98; found: C 52.65, H 3.97, N 7.98.

$\{[Cd(bpf)_2(NO_3)_2]\cdot PhNMe_2\}_n$ (2a): The general procedure described above was followed with *N*,*N*-dimethylaniline (0.24 mL, 1.9 mmol) to give the title compound as slightly yellow, prism-shaped crystals in 45% yield (14 mg). Elemental analysis calcd (%) for $C_{44}H_{35}CdF_8N_7O_6$ ($[Cd(bpf)_2(NO_3)_2]\cdot PhNMe_2$): C 51.70, H 3.45, N 9.59; found: C 51.69, H 3.45, N 9.50.

$\{[Cd(bpf)_2(NO_3)_2]\cdot p\text{-}C_6H_4Me_2\}_n$ (2b): The general procedure described above was followed with $Cd(NO_3)_2{\cdot}4H_2O$ (19 mg, 0.06 mmol) in H_2O (0.5 mL), bpf (40 mg, 0.12 mmol) in ethanol (2 mL), and *p*-xylene (0.47 mL, 3.8 mmol). After the mixture was allowed to stand for 24 h at room temperature, the title compound was obtained as colorless, prism-shaped crystals in 56% yield (34 mg). Elemental analysis calcd (%) for $C_{44}H_{34}CdF_8N_6O_6$ ($[Cd(bpf)_2(NO_3)_2]\cdot p\text{-}C_6H_4Me_2$): C 52.47, H 3.40, N 8.34; found: C 52.49, H 3.27, N 8.45.

$\{[Cd(bpf)_2(NO_3)_2]\cdot o\text{-}C_6H_4BrOMe\}_n$ (2c): The general procedure described above was followed with $Cd(NO_3)_2{\cdot}4H_2O$ (9.3 mg, 0.03 mmol) in H_2O (0.5 mL), bpf (20 mg, 0.06 mmol) in ethanol (2 mL), and *o*-bromoanisole (0.21 mL, 1.9 mmol). After the mixture was allowed to stand for 24 h at 5°C, the title compound was obtained as colorless, prism-shaped crystals in 45% yield (15 mg). Elemental analysis calcd (%) for $C_{43}H_{31}BrCdF_8N_6O_7$ ($[Cd(bpf)_2(NO_3)_2]\cdot o\text{-}C_6H_4BrOMe$): C 47.47, H 2.87, N 7.72; found: C 47.30, H 3.00, N 7.42.

$\{[Cd(bpf)_2(NO_3)_2]\cdot$naphthalene$\}_n$ (2d): The general procedure described above was followed with $Cd(NO_3)_2{\cdot}4H_2O$ (9.3 mg, 0.03 mmol) in H_2O (0.5 mL), bpf (20 mg, 0.06 mmol) in ethanol (2 mL), and a saturated ethanol solution of naphthalene (0.5 mL). After the mixture was allowed to stand for 48 h at room temperature, the title compound was obtained as colorless, prism-shaped crystals in 60% yield (18 mg). Elemental analysis calcd (%) for $C_{46}H_{32}CdF_8N_6O_6$ ($[Cd(bpf)_2(NO_3)_2]\cdot$naphthalene): C 53.68, H 3.13, N 8.17; found: C 53.51, H 2.94, N 8.10.

$\{[Cd(bpf)_2(NO_3)_2]\cdot(p\text{-}C_6H_4BrMe)_2\}_n$ (3): The general procedure described above was followed with *p*-bromotoluene (0.33 g, 1.9 mmol) in ethanol (0.5 mL). After the mixture was allowed to stand for 48 h at room temperature, the title compound was obtained as colorless, prism-shaped crystals in 21% yield (7.7 mg). Elemental analysis calcd (%) for $C_{50}H_{38}Br_2CdF_8N_6O_6$ ($[Cd(bpf)_2(NO_3)_2]\cdot(p\text{-}C_6H_4BrMe)_2$): C 48.31, H 3.08, N 6.76; found: C 48.04, H 2.79, N 6.84.

$\{[Cd(bpf)_2(NO_3)_2]\cdot(C_6H_6)_3\}_n$ (4): The general procedure described above was followed with benzene (0.17 mL, 1.9 mmol). After the mixture was allowed to stand for 48 h at room temperature, the title compound was obtained as colorless, prism-shaped crystals in 54% yield (18 mg). Elemental analysis calcd (%) for $C_{42}H_{30}CdF_8N_6O_6$ ($[Cd(bpf)_2(NO_3)_2]\cdot$(benzene)$_2$): C 54.53, H 3.43, N 7.95; found: C 54.21, H 3.66, N 7.82.

$\{[Cd(bpf)_2(NO_3)_2]\cdot(o\text{-}C_6H_4Me_2)_4\}_n$ (5a): The general procedure described above was followed with *o*-xylene (0.23 mL, 1.9 mmol). After the mixture was allowed to stand for 48 h at room temperature, the title compound was obtained as colorless, prism-shaped crystals in 48% yield (18.9 mg). Elemental analysis calcd (%) for $C_{64}H_{39}CdF_8N_6O_6$ ($[Cd(bpf)_2(NO_3)_2]\cdot(o\text{-}C_6H_4Me_2)_{3.5}$): C 60.40, H 4.67, N 6.60; found: C 60.51, H 4.87, N 6.48.

$\{[Cd(bpf)_2(NO_3)_2]\cdot(o\text{-}C_6H_4NH_2Me)_4\}_n$ (5b): The general procedure described above was followed with *o*-toluidine (0.20 mL, 1.9 mmol). After the mixture was allowed to stand for 48 h at room temperature, the title compound was obtained as colorless, prism-shaped crystals in 34% yield (13 mg). Elemental analysis calcd (%) for $C_{64}H_{60}CdF_8N_{10}O_6$ ($[Cd(bpf)_2(NO_3)_2]\cdot(o\text{-}C_6H_4NH_2Me)_4$): C 57.81, H 4.55, N 10.53; found: C 57.75, H 4.61, N 10.47.

$\{[Cd(bpf)_2(NO_3)_2]\cdot(PhOCOMe)_2\}_n$ (6a): The general procedure described above was followed with phenyl acetate (0.24 mL, 1.9 mmol). After the mixture was allowed to stand for 48 h at room temperature, the title compound was obtained as colorless, prism-shaped crystals in 73% yield (23 mg). Elemental analysis calcd (%) for $C_{52}H_{40}CdF_8N_6O_{10}$ ($[Cd(bpf)_2(NO_3)_2]\cdot($ PhOCOMe$)_2$): C 53.23, H 3.44, N 7.16; found: C 53.00, H 3.28, N 7.14.

$\{[Cd(bpf)_2(NO_3)_2]\cdot(m\text{-}C_6H_4Me_2)_2\}_n$ (6b): The general procedure described above was followed with *m*-xylene (0.23 mL, 1.9 mmol). After the mixture was allowed to stand for 48 h at room temperature, the title compound was obtained as colorless, prism-shaped crystals in 64% yield (21 mg). Elemental analysis calcd (%) for $C_{52}H_{40}CdF_8N_6O_{10}$ ($[Cd(bpf)_2(NO_3)_2]\cdot(m\text{-}C_6H_4Me_2)_2$): C 56.10, H 3.98, N 7.55; found: C 56.02, H 3.84, N 7.56.

$\{[Cd(bpf)_2(NO_3)_2]\cdot(PhNHMe)_2\}_n$ (6c): The general procedure described above was followed with *N*-methylaniline (0.21 mL, 1.9 mmol). After the mixture was allowed to stand for 48 h at room temperature, the title compound was obtained as light-brown, prism-shaped crystals in 66% yield (22 mg). Elemental analysis calcd (%) for $C_{50}H_{42}CdF_8N_8O_6$ ($[Cd(bpf)_2(NO_3)_2]\cdot(PhNHMe)_2$): C 53.84, H 3.80, N 10.05; found: C 53.89, H 3.48, N 10.02.

$\{[Cd(bpf)_2(NO_3)_2]\cdot(PhMe)_2\}_n$ (6d): The general procedure described above was followed with $Cd(NO_3)_2{\cdot}4H_2O$ (19 mg, 0.06 mmol) in H_2O (0.5 mL), bpf (40 mg, 0.12 mmol) in ethanol (2 mL), and toluene (0.41 mL, 3.8 mmol). The title compound was obtained as colorless,

prism-shaped crystals in 31% yield (21 mg). Elemental analysis calcd (%) for $C_{50}H_{40}CdF_8N_6O_6$ ($[Cd(bpf)_2(NO_3)_2]\cdot(PhMe)_2$): C 55.33, H 3.71, N 7.74; found: C 55.23, H 3.67, N 7.81.

$\{[Cd(bpf)_2(NO_3)_2]\cdot(biphenyl)_2\}_n$ (6e): The general procedure described above was followed with $Cd(NO_3)_2\cdot 4H_2O$ (9.3 mg, 0.03 mmol) in H_2O (0.25 mL), bpf (20 mg, 0.06 mmol) in ethanol (1 mL), and a saturated ethanol solution of biphenyl (0.5 mL). After the mixture was allowed to stand for 48 h at room temperature, the title compound was obtained as colorless, prism-shaped crystals in 43% yield (16 mg). Elemental analysis calcd (%) for $C_{60}H_{44}CdF_8N_6O_6$ ($[Cd(bpf)_2(NO_3)_2]\cdot(biphenyl)_2$): C 59.59, H 3.67, N 6.95; found: C 59.51, H 3.53, N 7.14.

$\{[Cd(bpf)_2(NO_3)_2]\cdot(PhCH_2OMe)_2\}_n$ (6f): The general procedure described above was followed with benzyl methyl ether (0.23 mL, 1.9 mmol). After the mixture was allowed to stand for 48 h at room temperature, the title compound was obtained as colorless, prism-shaped crystals in 60% yield (21 mg). Elemental analysis calcd (%) for $C_{52}H_{44}CdF_8N_6O_8$ ($[Cd(bpf)_2(NO_3)_2]\cdot(PhCH_2OMe)_2$): C 54.53, H 3.87, N 7.34; found: C 54.54, H 3.93, N 7.33.

$\{[Cd(bpf)_2(NO_3)_2]\cdot(PhEt)_2\}_n$ (6g): The general procedure described above was followed with ethylbenzene (0.23 mL, 1.9 mmol). After the mixture was allowed to stand for 48 h at room temperature, the title compound was obtained as colorless, prism-shaped crystals in 48% yield (16 mg). Elemental analysis calcd (%) for $C_{52}H_{44}CdF_8N_6O_6$ ($[Cd(bpf)_2(NO_3)_2]\cdot(PhEt)_2$): C 56.10, H 3.98, N 7.55; found: C 55.99, H 4.08, N 7.43.

$\{[Cd(bpf)_2(NO_3)_2]\cdot(PhCH(Me)=CH_2)_2\}_n$ (6h): The general procedure described above was followed with $Cd(NO_3)_2\cdot 4H_2O$ (9.3 mg, 0.03 mmol) in H_2O (0.5 mL), bpf (20 mg, 0.06 mmol) in ethanol (2 mL), and 2-phenylpropene (0.25 mL, 1.9 mmol). After the mixture was allowed to stand for 24 h at 5°C, the title compound was obtained as colorless, prism-shaped crystals in 57% yield (19 mg). Elemental analysis calcd (%) for $C_{52}H_{44}CdF_8N_6O_8$ ($[Cd(bpf)_2(NO_3)_2]\cdot(PhCH(Me)=CH_2)_2$): C 57.03, H 3.90, N 7.39; found: C 57.11, H 3.98, N 7.36.

$\{[Cd(bpfb)_2(NO_3)_2]\cdot(EtOH)_2\}_n$ (7): The general procedure described above was followed with $Cd(NO_3)_2\cdot 4H_2O$ (9.3 mg, 0.03 mmol) in H_2O (0.5 mL) and bpfb (29 mg, 0.06 mmol) in ethanol (2 mL). After the mixture was allowed to stand for 24 h at 5°C, the title compound was obtained as colorless, prism-shaped crystals in 38% yield (15 mg). Elemental analysis calcd (%) for $C_{52}H_{36}CdF_{16}N_6O_8$ ($[Cd(bpfb)_2(NO_3)_2]\cdot(EtOH)_2$): C 48.44, H 2.81, N 6.52; found: C 48.24, H 2.51, N 6.72.

$\{[Cd(bpfb)_2(NO_3)_2]\cdot(PhOCOMe)_2\}_n$ (8a): The general procedure described above was followed with $Cd(NO_3)_2\cdot 4H_2O$ (9.3 mg, 0.03 mmol) in H_2O (0.5 mL), bpfb (29 mg, 0.06 mmol) in ethanol (2 mL), and phenyl acetate (0.24 mL, 1.9 mmol). After the mixture was allowed to stand for 24 h at 5°C, the title compound was obtained as colorless, prism-shaped crystals in 66% yield (29 mg). Elemental analysis calcd (%) for $C_{64}H_{40}CdF_{16}N_6O_{10}$ ($[Cd(bpfb)_2(NO_3)_2]\cdot(PhOCOMe)_2$): C 52.31, H 2.74, N 5.72; found: C 52.27, H 2.63, N 5.76.

$\{[Cd(bpfb)_2(NO_3)_2]\cdot(PhNMe_2)_2\}_n$ (8b): The general procedure described above was followed with *N*,*N*-dimethylaniline (0.24 mL, 1.9 mmol). After the mixture was allowed to stand for 24 h at 5°C, the title compound was obtained as pale-yellow, prism-shaped crystals in 23% yield (9.9 mg). Elemental analysis calcd (%) for $C_{62}H_{46}CdF_{16}N_8O_6$ ($[Cd(bpfb)_2(NO_3)_2]\cdot(PhNMe_2)_2$): C 53.40, H 3.22, N 7.78; found: C 53.55, H 3.03, N 7.69.

$\{[Cd(bpfb)_2(NO_3)_2]\cdot(m\text{-}C_6H_4(OMe)_2)_2\}_n$ (8c): The general procedure described above was followed with *m*-dimethoxybenzene (0.25 mL, 1.9 mmol). After the mixture was allowed to stand for 24 h at 5°C, the title compound was obtained as colorless, prism-shaped crystals in 46% yield (20 mg). Elemental analysis calcd (%) for $C_{64}H_{44}CdF_{16}N_6O_{10}$ ($[Cd(bpfb)_2(NO_3)_2]\cdot(m\text{-}C_6H_4(OMe)_2)_2$): C 52.17, H 3.01, N 5.70; found: C 52.30, H 3.12, N 5.41.

$\{[Cd(bpfb)_2(NO_3)_2]\cdot(biphenyl)_2\}_n$ (8d): The general procedure described above was followed with a saturated ethanol solution of biphenyl (0.5 mL). After the mixture was allowed to stand for 48 h at room temperature, the title compound was obtained as colorless, prism-shaped crystals in 36% yield (17 mg). Elemental analysis calcd (%) for $C_{74}H_{51}CdF_{16}N_6O_{7.5}$ ($[Cd(bpfb)_2(NO_3)_2]\cdot(biphenyl)_2\cdot EtOH\cdot(H_2O)_{0.5}$): C 56.95, H 3.29, N 5.38; found: C 56.81, H 3.34, N 5.42.

$\{[Cd(bpfb)_2(NO_3)_2]\cdot(naphthalene)_2\}_n$ (8e): The general procedure described above was followed with $Cd(NO_3)_2\cdot 4H_2O$ (9.3 mg, 0.03 mmol) in H_2O (0.5 mL), bpfb (29 mg, 0.06 mmol) in ethanol (2 mL), and a saturated ethanol solution of naphthalene (0.5 mL). After the mixture was allowed to stand for 48 h at room temperature, the title compound was obtained as colorless, prism-shaped crystals in 50% yield (22 mg). Elemental analysis calcd (%) for $C_{68}H_{40}CdF_{16}N_6O_6$ ($[Cd(bpfb)_2(NO_3)_2]\cdot(naphthalene)_2$): C 56.19, H 2.77, N 5.78; found: C 56.12, H 2.42, N 5.72.

$\{[Cd(2,6\text{-}bpfn)_{1.5}(NO_3)_2]\cdot EtOH\}_n$ (9): The general procedure described above was followed with $Cd(NO_3)_2\cdot 4H_2O$ (9.3 mg, 0.03 mmol) in H_2O (0.5 mL) and 2,6-bpfn (25 mg, 0.06 mmol) in ethanol (2 mL). After the mixture was allowed to stand for 24 h at 5°C, the title compound was obtained as colorless, prism-shaped crystals in 60% yield (16 mg). Elemental analysis calcd (%) for $C_{35}H_{24}CdF_9N_5O_7$ ($[Cd(2,6\text{-}bpfn)_{1.5}(NO_3)_2]\cdot EtOH$): C 46.20, H 2.66, N 7.70; found: C 46.37, H 2.55, N 7.60.

$\{[Cd(2,6\text{-}bpfn)_2(NO_3)_2]\cdot(p\text{-}C_6H_4(OMe)_2)_2\}_n$ (10a): The general procedure described above was followed with $Cd(NO_3)_2\cdot 4H_2O$ (9.3 mg, 0.03 mmol) in H_2O (0.5 mL), 2,6-bpfn (25 mg, 0.06 mmol) in ethanol (2 mL), and *p*-dimethoxybenzene (0.26 g, 1.9 mmol) in ethanol (0.5 mL). After the mixture was allowed to stand for 24 h at 5°C, the title compound was obtained as colorless, prism-shaped crystals in 48% yield (20 mg). Elemental analysis calcd (%) for $C_{62}H_{50}CdF_{12}N_6O_{11}$ ($[Cd(2,6\text{-}bpfn)_2(NO_3)_2]\cdot(p\text{-}C_6H_4(OMe)_2)_2\cdot EtOH$): C 53.36, H 3.61, N 6.02; found: C 53.34, H 3.65, N 6.07.

$\{[Cd(2,6\text{-}bpfn)_2(NO_3)_2]\cdot(PhCOOMe)_2\}_n$ (10b): The general procedure described above was followed with methyl benzoate (0.24 mL, 1.9 mmol). After the mixture was allowed to stand for 24 h at 5°C, the title compound was obtained as colorless, prism-shaped crystals in 64% yield (27 mg). Elemental analysis calcd (%) for $C_{62}H_{46}CdF_{12}N_6O_{11}$ ($[Cd(2,6\text{-}bpfn)_2(NO_3)_2]\cdot(PhCOOMe)_2\cdot EtOH$): C 53.52, H 3.33, N 6.04; found: C 53.50, H 3.38, N 5.97.

$\{[Cd(2,6\text{-}bpfn)_2(NO_3)_2]\cdot(biphenyl)_2\}_n$ (10c): The general procedure described above was followed with a saturated ethanol solution of biphenyl (0.5 mL). After the mixture was allowed to stand for 24 h at 15°C, the title compound was obtained as colorless, prism-shaped crystals in 30% yield (13 mg). Elemental analysis calcd (%) for $C_{68}H_{44}CdF_{12}N_6O_6$ ($[Cd(2,6\text{-}bpfn)_2(NO_3)_2]\cdot(biphenyl)_2$): C 59.12, H 3.21, N 6.08; found: C 58.96, H 3.52, N 5.99.

$\{[Cd(2,6\text{-}bpfn)_2(NO_3)_2]\cdot(p\text{-}C_6H_4Me_2)_2\}_n$ (11a): The general procedure described above was followed with *p*-xylene (0.23 mL, 1.9 mmol). After the mixture was allowed to stand for 48 h at 5°C, the title compound was obtained as colorless, prism-shaped crystals in 54% yield (21 mg). Elemental analysis calcd (%) for $C_{60}H_{44}CdF_{12}N_6O_6$ ($[Cd(2,6\text{-}bpfn)_2(NO_3)_2]\cdot(p\text{-}C_6H_4Me_2)_2$): C 56.06, H 3.45, N 6.54; found: C 55.76, H 3.61, N 6.47.

$\{[Cd(2,6\text{-}bpfn)_2(NO_3)_2]\cdot(naphthalene)_2\}_n$ (11b): The general procedure described above was followed with a saturated ethanol solution of naphthalene (0.5 mL). After the mixture was allowed to stand for 48 h at room temperature, the title compound was obtained as colorless, prism-shaped crystals in 38% yield (15 mg). Elemental analysis calcd (%) for $C_{64}H_{40}CdF_{12}N_6O_6$ ($[Cd(2,6\text{-}bpfn)_2(NO_3)_2]\cdot(naphthalene)_2$): C 57.82, H 3.03, N 6.32; found: C 57.46, H 3.23, N 6.39.

$\{[Cd(2,6\text{-}bpfn)_2(NO_3)_2]\cdot(m\text{-}C_6H_4Me_2)_2\}_n$ (11c): The general procedure described above was followed with *m*-xylene (0.23 mL, 1.9 mmol). After the mixture was allowed to stand for 48 h at 5°C, the title compound was obtained as colorless, prism-shaped crystals in 38% yield (15 mg). Elemental analysis calcd (%) for $C_{60}H_{44}CdF_{12}N_6O_6$ ($[Cd(2,6\text{-}bpfn)_2(NO_3)_2]\cdot(m\text{-}C_6H_4Me_2)_2$): C 56.06, H 3.45, N 6.54; found: C 56.31, H 3.40, N 6.50.

$\{[Cd(2,6\text{-}bpfn)_2(NO_3)_2]\cdot(m\text{-}C_6H_4(OMe)_2)_2\}_n$ (11d): The general procedure described above was followed with *m*-dimethoxybenzene (0.25 mL, 1.9 mmol). After the mixture was allowed to stand for 48 h at 5°C, the title compound was obtained as colorless, prism-shaped crystals in 44% yield (18 mg). Elemental analysis calcd (%) for $C_{60}H_{44}CdF_{12}N_6O_{10}$ ($[Cd(2,6\text{-}bpfn)_2(NO_3)_2]\cdot(m\text{-}C_6H_4(OMe)_2)_2$): C 53.40, H 3.29, N 6.23; found: C 53.59, H 3.58, N 6.30.

$\{[Cd(2,6\text{-}bpfn)_2(NO_3)_2]\cdot(PhNMe_2)_2\}_n$ (11e): The general procedure described above was followed with *N*,*N*-dimethylaniline (0.24 mL,

1.9 mmol). After the mixture was allowed to stand for 48 h at 5 °C, the title compound was obtained as colorless, prism-shaped crystals in 42 % yield (17 mg). Elemental analysis calcd (%) for $C_{60}H_{46}CdF_{12}N_8O_6$ ([Cd(2,6-bpfn)$_2$(NO$_3$)$_2$]·(PhNMe$_2$)$_2$): C 54.78, H 3.52, N 8.53; found: C 54.53, H 3.72, N 8.38.

{[Cd(2,6-bpfn)$_2$(NO$_3$)$_2$]·(*p*-C$_6$H$_4$BrMe)$_2$}$_n$ (11 f): The general procedure described above was followed with *p*-bromotoluene (0.33 g, 1.9 mmol) in ethanol (0.5 mL). After the mixture was allowed to stand for 48 h at room temperature, the title compound was obtained as colorless, prism-shaped crystals in 48 % yield (21 mg). Elemental analysis calcd (%) for $C_{58}H_{40}Br_2CdF_{12}N_6O_7$ ([Cd(2,6-bpfn)$_2$(NO$_3$)$_2$]·(*p*-C$_6$H$_4$BrMe)$_2$·H$_2$O): C 48.61, H 2.81, N 5.86; found: C 48.93, H 2.89, N 5.68.

{[Cd(2,6-bpfn)$_2$(NO$_3$)$_2$]·(PhCH(Me)=CH$_2$)$_2$}$_n$ (11 g): The general procedure described above was followed with 2-phenylpropene (0.25 mL, 1.9 mmol). After the mixture was allowed to stand for 48 h at 5 °C, the title compound was obtained as colorless, prism-shaped crystals in 52 % yield (21 mg). Elemental analysis calcd (%) for $C_{62}H_{44}CdF_{12}N_6O_6$ ([Cd(2,6-bpfn)$_2$(NO$_3$)$_2$]·(PhCH(Me)=CH$_2$)$_2$): C 56.87, H 3.39, N 6.42; found: C 56.62, H 3.46, N 6.43.

{[Cd$_2$(2,6-bpfn)$_3$(NO$_3$)$_4$]·PhNHMe}$_n$ (12): The general procedure described above was followed with *N*-methylaniline (0.21 mL, 1.9 mmol). After the mixture was allowed to stand for 48 h at 5 °C, the title compound was obtained as light-brown, pillar-shaped crystals in 61 % yield (17 mg). Elemental analysis calcd (%) for $C_{73}H_{45}Cd_2F_{18}N_{12}O_{11}$ ([Cd$_2$(2,6-bpfn)$_3$(NO$_3$)$_4$]·PhNHMe): C 47.78, H 2.47, N 8.40; found: C 47.99, H 2.85, N 8.22.

{[Cd(2,7-bpfn)$_2$(NO$_3$)$_2$]·(*m*-C$_6$H$_4$(OMe)$_2$)$_2$}$_n$ (13): The general procedure described above was followed with Cd(NO$_3$)$_2$·4H$_2$O (9.3 mg, 0.03 mmol) in H$_2$O (0.25 mL), 2,7-bpfn (25 mg, 0.06 mmol) in ethanol (1 mL), and *m*-dimethoxybenzene (0.25 mL, 1.9 mmol). After the mixture was allowed to stand for 48 h at 5 °C, the title compound was obtained as colorless, plate-shaped crystals in 49 % yield (21 mg). Elemental analysis calcd (%) for $C_{64}H_{56}CdF_{12}N_6O_{12}$ ([Cd(2,7-bpfn)$_2$(NO$_3$)$_2$]·(*m*-C$_6$H$_4$(OMe)$_2$)$_2$·(EtOH)$_2$): C 53.32, H 3.92, N 5.83; found: C 53.19, H 4.01, N 5.79.

{[Cd(2,7-bpfn)$_2$(NO$_3$)$_2$]·(*m*-C$_6$H$_4$Me$_2$)$_2$}$_n$ (14 a): The general procedure described above was followed with Cd(NO$_3$)$_2$·4H$_2$O (9.3 mg, 0.03 mmol) in H$_2$O (0.4 mL), 2,7-bpfn (25 mg, 0.06 mmol) in ethanol (1.6 mL), and *m*-xylene (0.23 mL, 1.9 mmol). After the mixture was allowed to stand for 48 h at room temperature, the title compound was obtained as colorless, pillar-shaped crystals in 69 % yield (27 mg). Elemental analysis calcd (%) for $C_{60}H_{44}CdF_{12}N_6O_6$ ([Cd(2,7-bpfn)$_2$(NO$_3$)$_2$]·(*m*-C$_6$H$_4$Me$_2$)$_2$): C 56.06, H 3.45, N 6.54; found: C 56.14, H 3.58, N 6.55.

{[Cd(2,7-bpfn)$_2$(NO$_3$)$_2$]·(PhOCOMe)$_2$}$_n$ (14 b): The general procedure described above was followed with Cd(NO$_3$)$_2$·4H$_2$O (9.3 mg, 0.03 mmol) in H$_2$O (0.2 mL), 2,7-bpfn (25 mg, 0.06 mmol) in ethanol (0.8 mL), and phenyl acetate (0.24 mL, 1.9 mmol). After the mixture was allowed to stand for 48 h at 5 °C, the title compound was obtained as colorless, pillar-shaped crystals in 19 % yield (7.8 mg). Elemental analysis calcd (%) for $C_{60}H_{40}CdF_{12}N_6O_{10}$ ([Cd(2,7-bpfn)$_2$(NO$_3$)$_2$]·(PhOCOMe)$_2$): C 53.56, H 3.00, N 6.25; found: C 53.56, H 3.09, N 6.28.

X-ray structure determinations: The data for all the structures were measured with a Bruker SMART/CCD diffractometer (Mo$_{K\alpha}$ radiation, λ = 0.71073 Å) by the ω–2θ scan technique using frames of 0.3° oscillation. An empirical absorption correction was applied using SADABS. All the structures were solved by direct methods and refined by full-matrix least-squares against F^2 of all data using the SHELXTL program package. The positions of the hydrogen atoms were generated geometrically, assigned isotropic thermal parameters, and allowed to ride on their respective parent atoms before the final cycle of least-squares refinements.

X-ray structural data for 1a: $C_{188}H_{168}Cd_4F_{32}N_{24}O_{28}$, M_r = 4269.06, monoclinic, space group *P*2/*n*, a = 13.0030(9), b = 16.8653(12), c = 21.5855(15) Å, β = 94.5690(10)°, V = 4718.6(6) Å^3, T = 173 K, Z = 1, ρ_{calcd} = 1.502 g cm^{-3}, $2\theta_{max}$ = 28.01°, μ(Mo$_{K\alpha}$) = 0.551 mm^{-1}, 30313 reflections were collected of which 11146 were unique (R_{int} = 0.0295), 7240 observed reflections ($I > 2\sigma(I)$), 637 parameters, final R_1 = 0.0509, wR_2 = 0.1449.

X-ray structural data for 1b: $C_{184}H_{160}Cd_4F_{32}N_{24}O_{28}$, M_r = 4212.96, monoclinic, space group *P*2/*n*, a = 12.976(2), b = 16.741(3), c = 21.619(4) Å, β = 93.723(3)°, V = 4686.5(14) Å^3, T = 173 K, Z = 1, ρ_{calcd} = 1.493 g cm^{-3}, $2\theta_{max}$ = 28.03°, μ(Mo$_{K\alpha}$) = 0.554 mm^{-1}, 29661 reflections were collected of which 10865 were unique (R_{int} = 0.0196), 7867 observed reflections ($I > 2\sigma(I)$), 669 parameters, final R_1 = 0.0581, wR_2 = 0.1509.

X-ray structural data for 2a: $C_{44}H_{35}CdF_8N_7O_6$, M_r = 1022.19, triclinic, space group $P\bar{1}$, a = 10.202(5), b = 10.333(5), c = 10.717(5) Å, α = 76.981(5)°, β = 72.501(5)°, γ = 80.762(5)°, V = 1044.5(9) Å^3, T = 173 K, Z = 1, ρ_{calcd} = 1.625 g cm^{-3}, $2\theta_{max}$ = 27.99°, μ(Mo$_{K\alpha}$) = 0.618 mm^{-1}, 6768 reflections were collected of which 4690 were unique (R_{int} = 0.0110), 4468 observed reflections ($I > 2\sigma(I)$), 340 parameters, final R_1 = 0.0466, wR_2 = 0.1312.

X-ray structural data for 2b $C_{44}H_{34}CdF_8N_6O_6$, M_r = 1007.17, triclinic, space group $P\bar{1}$, a = 10.363(5), b = 10.392(5), c = 10.412(5) Å, α = 73.869(5)°, β = 80.082(5)°, γ = 79.906(5)°, V = 1051.4(9) Å^3, T = 173 K, Z = 1, ρ_{calcd} = 1.591 g cm^{-3}, $2\theta_{max}$ = 28.03°, μ(Mo$_{K\alpha}$) = 0.612 mm^{-1}, 6695 reflections were collected of which 4688 were unique (R_{int} = 0.0121), 4543 observed reflections ($I > 2\sigma(I)$), 295 parameters, final R_1 = 0.0254, wR_2 = 0.0654.

X-ray structural data for 2c: $C_{43}H_{31}BrCdF_8N_6O_7$, M_r = 1088.05, triclinic, space group $P\bar{1}$, a = 10.129(2), b = 10.245(2), c = 21.438(4) Å, α = 77.169(3)°, β = 78.687(4)°, γ = 83.771(4)°, V = 2122.0(8) Å^3, T = 173 K, Z = 2, ρ_{calcd} = 1.703 g cm^{-3}, $2\theta_{max}$ = 28.01°, μ(Mo$_{K\alpha}$) = 1.550 mm^{-1}, 13391 reflections were collected of which 9407 were unique (R_{int} = 0.0214), 8451 observed reflections ($I > 2\sigma(I)$), 595 parameters, final R_1 = 0.0435, wR_2 = 0.1259.

X-ray structural data for 2d: $C_{138}H_{96}Cd_3F_{24}N_{18}O_{18}$, M_r = 3087.53, triclinic, space group $P\bar{1}$, a = 10.1585(15), b = 10.1852(15), c = 31.774(5) Å, α = 82.814(4)°, β = 80.953(3)°, γ = 84.325(3)°, V = 3210.6(8) Å^3, T = 298 K, Z = 1, ρ_{calcd} = 1.597 g cm^{-3}, $2\theta_{max}$ = 28.03°, μ(Mo$_{K\alpha}$) = 0.603 mm^{-1}, 33071 reflections were collected of which 15328 were unique (R_{int} = 0.0418), 7333 observed reflections ($I > 2\sigma(I)$), 907 parameters, final R_1 = 0.0500, wR_2 = 0.0850.

X-ray structural data for 3: $C_{50}H_{38}Br_2CdF_8N_6O_6$, M_r = 1243.08, triclinic, space group $P\bar{1}$, a = 10.4266(16), b = 14.988(2), c = 16.557(2) Å, α = 85.496(3)°, β = 89.673(3)°, γ = 81.114(3)°, V = 2548.3(6) Å^3, T = 173 K, Z = 2, ρ_{calcd} = 1.620 g cm^{-3}, $2\theta_{max}$ = 28.03°, μ(Mo$_{K\alpha}$) = 2.080 mm^{-1}, 16559 reflections were collected of which 11446 were unique (R_{int} = 0.0216), 8686 observed reflections ($I > 2\sigma(I)$), 691 parameters, final R_1 = 0.0579, wR_2 = 0.1643.

X-ray structural data for 4: $C_{54}H_{42}CdF_8N_6O_6$, M_r = 1135.34, monoclinic, space group $P2_1/n$, a = 17.427(2), b = 15.031(2), c = 19.413(3) Å, β = 97.567(3)°, V = 5040.7(12) Å^3, T = 173 K, Z = 4, ρ_{calcd} = 1.496 g cm^{-3}, $2\theta_{max}$ = 28.03°, μ(Mo$_{K\alpha}$) = 0.520 mm^{-1}, 32438 reflections were collected of which 11795 were unique (R_{int} = 0.0548), 7286 observed reflections ($I > 2\sigma(I)$), 772 parameters, final R_1 = 0.0405, wR_2 = 0.0744.

X-ray structural data for 5a: $C_{68}H_{64}CdF_8N_6O_6$, M_r = 1325.65, monoclinic, space group $P2_1/n$, a = 13.582(2), b = 29.425(5), c = 16.240(3) Å, β = 106.624(3)°, V = 6219.0(17) Å^3, T = 173 K, Z = 4, ρ_{calcd} = 1.416 g cm^{-3}, $2\theta_{max}$ = 28.05°, μ(Mo$_{K\alpha}$) = 0.433 mm^{-1}, 40361 reflections were collected of which 14721 were unique (R_{int} = 0.0555), 8469 observed reflections ($I > 2\sigma(I)$), 802 parameters, final R_1 = 0.0506, wR_2 = 0.1241.

X-ray structural data for 5b: $C_{64}H_{60}CdF_8N_{10}O_6$, M_r = 1329.62, monoclinic, space group $P2_1/n$, a = 13.3493(10), b = 29.331(2), c = 16.2557(13) Å, β = 106.792(2)°, V = 6093.5(8) Å^3, T = 153 K, Z = 4, ρ_{calcd} = 1.449 g cm^{-3}, $2\theta_{max}$ = 28.03°, μ(Mo$_{K\alpha}$) = 0.444 mm^{-1}, 40489 reflections were collected of which 14605 were unique (R_{int} = 0.1038), 6856 observed reflections ($I > 2\sigma(I)$), 686 parameters, final R_1 = 0.1236, wR_2 = 0.3322.

X-ray structural data for 6a: $C_{52}H_{40}CdF_8N_6O_{10}$, M_r = 1173.30, monoclinic, space group *C*2/*c*, a = 17.902(5), b = 18.977(5), c = 16.758(5) Å, β = 119.512(5)°, V = 4954(2) Å^3, T = 173 K, Z = 4, ρ_{calcd} = 1.573 g cm^{-3}, $2\theta_{max}$ = 28.01°, μ(Mo$_{K\alpha}$) = 0.538 mm^{-1}, 15857 reflections were collected of which 5823 were unique (R_{int} = 0.0134), 5455 observed reflections ($I > 2\sigma(I)$), 348 parameters, final R_1 = 0.0256, wR_2 = 0.0672.

X-ray structural data for 6b: $C_{52}H_{44}CdF_8N_6O_6$, M_r = 1113.33, monoclinic, space group *C*2/*c*, a = 17.9094(10), b = 19.2662(11), c = 16.5765(9) Å, β =

122.0680(10)°, $V=4846.9(5)$ Å^3, $T=173$ K, $Z=4$, $\rho_{calcd}=1.526$ g cm^{-3}, $2\theta_{max}=28.05°$, $\mu(Mo_{K\alpha})=0.539$ mm^{-1}, 15401 reflections were collected of which 5674 were unique ($R_{int}=0.0146$), 5230 observed reflections ($I>2\sigma(I)$), 457 parameters, final $R_1=0.0255$, w$R_2=0.0724$.

X-ray structural data for 6c: $C_{50}H_{42}CdF_8N_8O_6$, $M_r=1115.32$, monoclinic, space group $C2/c$, $a=17.170(5)$, $b=19.060(5)$, $c=16.690(5)$ Å, $\beta=118.593(5)°$, $V=4796(2)$ Å^3, $T=173$ K, $Z=4$, $\rho_{calcd}=1.545$ g cm^{-3}, $2\theta_{max}=28.02°$, $\mu(Mo_{K\alpha})=0.546$ mm^{-1}, 15195 reflections were collected of which 5628 were unique ($R_{int}=0.0181$), 5038 observed reflections ($I>2\sigma(I)$), 330 parameters, final $R_1=0.0297$, w$R_2=0.0836$.

X-ray structural data for 6d: $C_{50}H_{40}CdF_8N_6O_6$, $M_r=1085.28$, monoclinic, space group $C2/c$, $a=17.535(3)$, $b=19.296(3)$, $c=16.240(2)$ Å, $\beta=119.822(2)°$, $V=4767.2(12)$ Å^3, $T=173$ K, $Z=4$, $\rho_{calcd}=1.512$ g cm^{-3}, $2\theta_{max}=28.00°$, $\mu(Mo_{K\alpha})=0.546$ mm^{-1}, 15091 reflections were collected of which 5585 were unique ($R_{int}=0.0192$), 5045 observed reflections ($I>2\sigma(I)$), 389 parameters, final $R_1=0.0322$, w$R_2=0.0883$.

X-ray structural data for 6e: $C_{60}H_{44}CdF_8N_6O_6$, $M_r=1209.41$, monoclinic, space group $C2/c$, $a=18.9509(17)$, $b=19.1159(17)$, $c=17.1188(16)$ Å, $\beta=121.116(2)°$, $V=5309.3(8)$ Å^3, $T=200$ K, $Z=4$, $\rho_{calcd}=1.513$ g cm^{-3}, $2\theta_{max}=27.52°$, $\mu(Mo_{K\alpha})=0.499$ mm^{-1}, 19357 reflections were collected of which 6097 were unique ($R_{int}=0.0235$), 5211 observed reflections ($I>2\sigma(I)$), 454 parameters, final $R_1=0.0332$, w$R_2=0.0777$.

X-ray structural data for 6f: $C_{52}H_{44}CdF_8N_6O_8$, $M_r=1145.33$, triclinic, space group $P\bar{1}$, $a=13.047(12)$, $b=13.279(12)$, $c=17.377(15)$ Å, $\alpha=67.645(14)°$, $\beta=64.369(15)°$, $\gamma=87.266(17)°$, $V=2486(4)$ Å^3, $T=173$ K, $Z=2$, $\rho_{calcd}=1.530$ g cm^{-3}, $2\theta_{max}=28.17°$, $\mu(Mo_{K\alpha})=0.531$ mm^{-1}, 15776 reflections were collected of which 11010 were unique ($R_{int}=0.0763$), 8214 observed reflections ($I>2\sigma(I)$), 676 parameters, final $R_1=0.1397$, w$R_2=0.3755$.

X-ray structural data for 6g: $C_{52}H_{44}CdF_8N_6O_6$, $M_r=1113.33$, triclinic, space group $P\bar{1}$, $a=12.9299(18)$, $b=13.1800(18)$, $c=16.971(2)$ Å, $\alpha=65.036(2)°$, $\beta=69.116(2)°$, $\gamma=86.222(3)°$, $V=2437.5(6)$ Å^3, $T=173$ K, $Z=2$, $\rho_{calcd}=1.517$ g cm^{-3}, $2\theta_{max}=27.99°$, $\mu(Mo_{K\alpha})=0.536$ mm^{-1}, 15872 reflections were collected of which 10974 were unique ($R_{int}=0.0129$), 9595 observed reflections ($I>2\sigma(I)$), 754 parameters, final $R_1=0.0271$, w$R_2=0.0674$.

X-ray structural data for 6h: $C_{108}H_{64}Cd_2F_{16}N_{12}O_{12}$, $M_r=2250.51$, monoclinic, space group $P2_1/c$, $a=17.037(3)$, $b=19.255(3)$, $c=29.997(5)$ Å, $\beta=90.922(5)°$, $V=9839(3)$ Å^3, $T=173$ K, $Z=4$, $\rho_{calcd}=0.532$ g cm^{-3}, $2\theta_{max}=27.51°$, $\mu(Mo_{K\alpha})=0.532$ mm^{-1}, 71258 reflections were collected of which 22527 were unique ($R_{int}=0.0419$), 12425 observed reflections ($I>2\sigma(I)$), 1418 parameters, final $R_1=0.0423$, w$R_2=0.1001$.

X-ray structural data for 7: $C_{52}H_{36}CdF_{16}N_6O_8$, $M_r=1289.27$, monoclinic, space group $P2_1/c$, $a=9.7535(17)$, $b=15.049(3)$, $c=35.195(6)$ Å, $\beta=95.855(3)°$, $V=5139.1(16)$ Å^3, $T=173$ K, $Z=4$, $\rho_{calcd}=1.666$ g cm^{-3}, $2\theta_{max}=28.05°$, $\mu(Mo_{K\alpha})=0.545$ mm^{-1}, 32504 reflections were collected of which 12059 were unique ($R_{int}=0.0303$), 8445 observed reflections ($I>2\sigma(I)$), 794 parameters, final $R_1=0.0600$, w$R_2=0.1629$.

X-ray structural data for 8a: $C_{64}H_{40}CdF_{16}N_6O_{10}$, $M_r=1469.42$, orthorhombic, space group $Pccn$, $a=17.048(3)$, $b=20.897(3)$, $c=16.446(3)$ Å, $V=5859.0(16)$ Å^3, $T=173$ K, $Z=4$, $\rho_{calcd}=1.666$ g cm^{-3}, $2\theta_{max}=28.04°$, $\mu(Mo_{K\alpha})=0.492$ mm^{-1}, 36331 reflections were collected of which 6978 were unique ($R_{int}=0.0368$), 5187 observed reflections ($I>2\sigma(I)$), 438 parameters, final $R_1=0.0334$, w$R_2=0.0767$.

X-ray structural data for 8b: $C_{64}H_{46}CdF_{16}N_8O_6$, $M_r=1439.49$, orthorhombic, space group $Pccn$, $a=17.079(3)$, $b=21.562(3)$, $c=16.213(3)$ Å, $V=5970.4(16)$ Å^3, $T=173$ K, $Z=4$, $\rho_{calcd}=1.601$ g cm^{-3}, $2\theta_{max}=28.02°$, $\mu(Mo_{K\alpha})=0.477$ mm^{-1}, 36740 reflections were collected of which 7103 were unique ($R_{int}=0.0386$), 4883 observed reflections ($I>2\sigma(I)$), 497 parameters, final $R_1=0.0311$, w$R_2=0.0666$.

X-ray structural data for 8c: $C_{64}H_{44}CdF_{16}N_6O_{10}$, $M_r=1473.45$, orthorhombic, space group $Pccn$, $a=16.9863(11)$, $b=20.7220(13)$, $c=16.8879(10)$ Å, $V=5944.4(6)$ Å^3, $T=173$ K, $Z=4$, $\rho_{calcd}=1.646$ g cm^{-3}, $2\theta_{max}=28.01°$, $\mu(Mo_{K\alpha})=0.485$ mm^{-1}, 36474 reflections were collected of which 7132 were unique ($R_{int}=0.0360$), 5308 observed reflections ($I>2\sigma(I)$), 438 parameters, final $R_1=0.0481$, w$R_2=0.1358$.

X-ray structural data for 8d: $C_{148}H_{102}Cd_2F_{32}N_{12}O_{15}$, $M_r=3121.22$, orthorhombic, space group $Pcca$, $a=24.927(4)$, $b=17.262(3)$, $c=16.278(2)$ Å, $V=7004.2(17)$ Å^3, $T=173$ K, $Z=2$, $\rho_{calcd}=1.480$ g cm^{-3}, $2\theta_{max}=28.04°$, $\mu(Mo_{K\alpha})=0.414$ mm^{-1}, 43283 reflections were collected of which 8387 were unique ($R_{int}=0.0600$), 5269 observed reflections ($I>2\sigma(I)$), 519 parameters, final $R_1=0.0484$, w$R_2=0.1050$.

X-ray structural data for 8e: $C_{68}H_{44}CdF_{16}N_6O_6$, $M_r=1457.49$, monoclinic, space group Cc, $a=22.225(4)$, $b=16.876(3)$, $c=16.959(3)$ Å, $\beta=107.663(3)°$, $V=6060.7(16)$ Å^3, $T=173$ K, $Z=4$, $\rho_{calcd}=1.597$ g cm^{-3}, $2\theta_{max}=28.02°$, $\mu(Mo_{K\alpha})=0.470$ mm^{-1}, 19394 reflections were collected of which 9503 were unique ($R_{int}=0.0306$), 7695 observed reflections ($I>2\sigma(I)$), 875 parameters, final $R_1=0.0352$, w$R_2=0.0818$.

X-ray structural data for 9: $C_{35}H_{24}CdF_9N_5O_7$, $M_r=909.99$, triclinic, space group $P\bar{1}$, $a=11.0195(16)$, $b=12.3205(18)$, $c=13.694(2)$ Å, $\alpha=109.396(3)°$, $\beta=96.894(3)°$, $\gamma=97.120(3)°$, $V=1714.1(4)$ Å^3, $T=173$ K, $Z=2$, $\rho_{calcd}=1.763$ g cm^{-3}, $2\theta_{max}=28.02°$, $\mu(Mo_{K\alpha})=0.745$ mm^{-1}, 11257 reflections were collected of which 7761 were unique ($R_{int}=0.0171$), 7175 observed reflections ($I>2\sigma(I)$), 514 parameters, final $R_1=0.0662$, w$R_2=0.1811$.

X-ray structural data for 10a: $C_{62}H_{50}CdF_{12}N_6O_{11}$, $M_r=1395.48$, monoclinic, space group $C2/c$, $a=31.851(2)$, $b=13.6044(9)$, $c=14.5181(10)$ Å, $\beta=113.1370(10)°$, $V=5785.0(7)$ Å^3, $T=153$ K, $Z=4$, $\rho_{calcd}=1.602$ g cm^{-3}, $2\theta_{max}=28.01°$, $\mu(Mo_{K\alpha})=0.485$ mm^{-1}, 18892 reflections were collected of which 6928 were unique ($R_{int}=0.0295$), 5819 observed reflections ($I>2\sigma(I)$), 420 parameters, final $R_1=0.0489$, w$R_2=0.1392$.

X-ray structural data for 10b: $C_{62}H_{46}CdF_{12}N_6O_{11}$, $M_r=1391.45$, monoclinic, space group $C2/c$, $a=28.8753(16)$, $b=13.9207(8)$, $c=15.2183(9)$ Å, $\beta=111.8580(10)°$, $V=5677.4(6)$ Å^3, $T=153$ K, $Z=4$, $\rho_{calcd}=1.628$ g cm^{-3}, $2\theta_{max}=28.05°$, $\mu(Mo_{K\alpha})=0.494$ mm^{-1}, 18709 reflections were collected of which 6831 were unique ($R_{int}=0.0367$), 5082 observed reflections ($I>2\sigma(I)$), 420 parameters, final $R_1=0.0757$, w$R_2=0.2160$.

X-ray structural data for 10c: $C_{68}H_{44}CdF_{12}N_6O_6$, $M_r=1381.49$, triclinic, space group $P\bar{1}$, $a=11.289(3)$, $b=16.583(4)$, $c=18.834(5)$ Å, $\alpha=78.838(4)°$, $\beta=82.185(4)°$, $\gamma=84.608(5)°$, $V=3418.8(15)$ Å^3, $T=153$ K, $Z=2$, $\rho_{calcd}=1.342$ g cm^{-3}, $2\theta_{max}=28.15°$, $\mu(Mo_{K\alpha})=0.405$ mm^{-1}, 20905 reflections were collected of which 14704 were unique ($R_{int}=0.0533$), 9255 observed reflections ($I>2\sigma(I)$), 943 parameters, final $R_1=0.0977$, w$R_2=0.2571$.

X-ray structural data for 11a: $C_{60}H_{44}CdF_{12}N_6O_6$, $M_r=1285.41$, orthorhombic, space group $Pnnn$, $a=13.5217(13)$, $b=15.6921(16)$, $c=26.700(3)$ Å, $V=5665.4(10)$ Å^3, $T=153$ K, $Z=4$, $\rho_{calcd}=1.507$ g cm^{-3}, $2\theta_{max}=28.03°$, $\mu(Mo_{K\alpha})=0.482$ mm^{-1}, 35190 reflections were collected of which 6799 were unique ($R_{int}=0.0807$), 2950 observed reflections ($I>2\sigma(I)$), 387 parameters, final $R_1=0.0419$, w$R_2=0.0989$.

X-ray structural data for 11b: $C_{64}H_{44}CdF_{12}N_6O_6$, $M_r=1333.45$, orthorhombic, space group $Pnnn$, $a=13.380(3)$, $b=15.567(4)$, $c=27.205(6)$ Å, $V=5666(2)$ Å^3, $T=173$ K, $Z=4$, $\rho_{calcd}=1.563$ g cm^{-3}, $2\theta_{max}=28.02°$, $\mu(Mo_{K\alpha})=0.485$ mm^{-1}, 34830 reflections were collected of which 6764 were unique ($R_{int}=0.0466$), 4286 observed reflections ($I>2\sigma(I)$), 443 parameters, final $R_1=0.0499$, w$R_2=0.1267$.

X-ray structural data for 11c: $C_{60}H_{44}CdF_{12}N_6O_6$, $M_r=1285.41$, orthorhombic, space group $Pnnn$, $a=13.4802(8)$, $b=15.6560(9)$, $c=27.0214(16)$ Å, $V=5702.8(6)$ Å^3, $T=173$ K, $Z=4$, $\rho_{calcd}=1.497$ g cm^{-3}, $2\theta_{max}=28.00°$, $\mu(Mo_{K\alpha})=0.479$ mm^{-1}, 35219 reflections were collected of which 6829 were unique ($R_{int}=0.0253$), 4517 observed reflections ($I>2\sigma(I)$), 355 parameters, final $R_1=0.0617$, w$R_2=0.2025$.

X-ray structural data for 11d: $C_{60}H_{44}CdF_{12}N_6O_{10}$, $M_r=1349.41$, orthorhombic, space group $Pnnn$, $a=13.846(5)$, $b=15.451(5)$, $c=26.658(5)$ Å, $V=5703(3)$ Å^3, $T=153$ K, $Z=4$, $\rho_{calcd}=1.572$ g cm^{-3}, $2\theta_{max}=28.05°$, $\mu(Mo_{K\alpha})=0.488$ mm^{-1}, 35341 reflections were collected of which 6855 were unique ($R_{int}=0.0571$), 3356 observed reflections ($I>2\sigma(I)$), 393 parameters, final $R_1=0.0643$, w$R_2=0.1808$.

X-ray structural data for 11e: $C_{60}H_{46}CdF_{12}N_8O_6$, $M_r=1315.45$, orthorhombic, space group $Pnnn$, $a=13.451(5)$, $b=15.719(5)$, $c=26.935(5)$ Å, $V=5695(3)$ Å^3, $T=153$ K, $Z=4$, $\rho_{calcd}=1.534$ g cm^{-3}, $2\theta_{max}=28.03°$, $\mu(Mo_{K\alpha})=0.482$ mm^{-1}, 34343 reflections were collected of which 6804

were unique ($R_{int}=0.0638$), 4189 observed reflections ($I>2\sigma(I)$), 369 parameters, final $R_1=0.1436$, w$R_2=0.3028$.

X-ray structural data for 11f: $C_{58}H_{40}Br_2CdF_{12}N_6O_7$, $M_r=1433.18$, orthorhombic, space group *Pnnn*, $a=13.3884(16)$, $b=15.8530(19)$, $c=26.729(3)$ Å, $V=5673.0(12)$ Å^3, $T=153$ K, $Z=4$, $\rho_{calcd}=1.678$ g cm^{-3}, $2\theta_{max}=28.04°$, $\mu(Mo_{K\alpha})=1.892$ mm^{-1}, 36143 reflections were collected of which 6875 were unique ($R_{int}=0.0404$), 4357 observed reflections ($I>2\sigma(I)$), 386 parameters, final $R_1=0.0573$, w$R_2=0.1758$.

X-ray structural data for 11g: $C_{62}H_{44}CdF_{12}N_6O_6$, $M_r=1309.43$, orthorhombic, space group *Pnnn*, $a=13.494(5)$, $b=15.664(5)$, $c=26.830(5)$ Å, $V=5671(3)$ Å^3, $T=153$ K, $Z=4$, $\rho_{calcd}=1.534$ g cm^{-3}, $2\theta_{max}=28.04°$, $\mu(Mo_{K\alpha})=0.483$ mm^{-1}, 34989 reflections were collected of which 6824 were unique ($R_{int}=0.0478$), 3837 observed reflections ($I>2\sigma(I)$), 443 parameters, final $R_1=0.0708$, w$R_2=0.1684$.

X-ray structural data for 12: $C_{73}H_{47}Cd_2F_{18}N_{11}O_{13}$, $M_r=1853.02$, monoclinic, space group $P2_1/n$, $a=8.864(5)$, $b=28.744(5)$, $c=13.854(5)$ Å, $\beta=90.858(5)°$, $V=3529(2)$ Å^3, $T=153$ K, $Z=2$, $\rho_{calcd}=1.744$ g cm^{-3}, $2\theta_{max}=28.02°$, $\mu(Mo_{K\alpha})=0.725$ mm^{-1}, 22329 reflections were collected of which 8160 were unique ($R_{int}=0.0279$), 5850 observed reflections ($I>2\sigma(I)$), 550 parameters, final $R_1=0.0549$, w$R_2=0.1473$.

X-ray structural data for 13: $C_{64}H_{56}CdF_{12}N_6O_{12}$, $M_r=1441.55$, monoclinic, space group *C*2/*c*, $a=31.552(5)$, $b=13.533(2)$, $c=17.318(3)$ Å, $\beta=121.816(2)°$, $V=6283.8(17)$ Å^3, $T=173$ K, $Z=4$, $\rho_{calcd}=1.524$ g cm^{-3}, $2\theta_{max}=28.11°$, $\mu(Mo_{K\alpha})=0.450$ mm^{-1}, 19868 reflections were collected of which 7359 were unique ($R_{int}=0.0249$), 5828 observed reflections ($I>2\sigma(I)$), 448 parameters, final $R_1=0.0386$, w$R_2=0.1002$.

X-ray structural data for 14a: $C_{60}H_{44}CdF_{12}N_6O_6$, $M_r=1285.41$, monoclinic, space group $P2_1/c$, $a=8.1700(13)$, $b=20.445(3)$, $c=16.354(3)$ Å, $\beta=100.204(3)°$, $V=2688.6(7)$ Å^3, $T=153$ K, $Z=2$, $\rho_{calcd}=1.588$ g cm^{-3}, $2\theta_{max}=27.90°$, $\mu(Mo_{K\alpha})=0.508$ mm^{-1}, 17157 reflections were collected of which 6273 were unique ($R_{int}=0.0273$), 4662 observed reflections ($I>2\sigma(I)$), 449 parameters, final $R_1=0.0271$, w$R_2=0.0604$.

X-ray structural data for 14b: $C_{120}H_{80}Cd_2F_{24}N_{12}O_{20}$, $M_r=2690.76$, monoclinic, space group *Cc*, $a=16.286(2)$, $b=40.817(5)$, $c=16.875(2)$ Å, $\beta=99.467(2)°$, $V=11065(2)$ Å^3, $T=153$ K, $Z=4$, $\rho_{calcd}=1.615$ g cm^{-3}, $2\theta_{max}=27.99°$, $\mu(Mo_{K\alpha})=0.503$ mm^{-1}, 30648 reflections were collected of which 19523 were unique ($R_{int}=0.0239$), 13543 observed reflections ($I>2\sigma(I)$), 1604 parameters, final $R_1=0.0402$, w$R_2=0.0843$.

CCDC-282132 (**1a**), -282126 (**1b**), -282130 (**2a**), -282128 (**2b**), -282131 (**2c**), -282125 (**2d**), -282127 (**3**), -282129 (**4**), -282133 (**5a**), -282134 (**5b**), -282140 (**6a**), -282141 (**6b**), -282138 (**6c**), -282142 (**6d**), -282137 (**6e**), -282143 (**6f**), -282144 (**6g**), -282135 (**6h**), -282150 (**7**), -282147 (**8a**), -282149 (**8b**), -282148 (**8c**), -282146 (**8d**), -282145 (**8e**), -282159 (**9**), -282158 (**10a**), -282161 (**10b**), -282157 (**10c**), -282164 (**11a**), -282162 (**11b**), -282163 (**11c**), -282160 (**11d**), -282156 (**11e**), -282155 (**11f**), -282171 (**11g**), -282170 (**12**), -282167 (**13**), -282166 (**14a**), and -282169 (**14b**) contain the supplementary crystallographic data for this paper. These data can be obtained free of charge from the Cambridge Crystallographic Data Centre via www.ccdc.cam.ac.uk/data_request/cif.

Attempts to obtain clathrate networks from bpb: The reaction of $Cd(NO_3)_2\cdot 4H_2O$ (9.3 mg, 0.03 mmol) in H_2O (0.25 mL), bpb (16 mg, 0.06 mmol) in ethanol (1 mL), and phenyl acetate (0.24 mL, 1.9 mmol) was attempted under the same reaction conditions as for bpf. After the mixture was allowed to stand for 48 h at room temperature, $[Cd(bpb)_{1.5}(NO_3)_2]_n$ was obtained as colorless, pillar-shaped crystals in 31% yield (6.1 mg). The structure was identified by preliminary X-ray measurement of a single crystal to determine the unit cell parameters and space group. Elemental analysis calcd (%) for $C_{27}H_{24}CdN_5O_6$ ($[Cd(bpb)_{1.5}(NO_3)_2]_n$): C 51.73, H 3.86, N 11.17; found: C 51.71, H 3.20, N 11.05. The same reaction in the presence of *N*,*N*-dimethylaniline or *m*-xylene also gave $[Cd(bpb)_{1.5}(NO_3)_2]_n$ in 33% (6.2 mg) and 32% (6.1 mg) yield, respectively. These structures were identified by preliminary X-ray measurements of single crystals.

Acknowledgments

We thank Dr. Masaru Aoyagi and Dr. Kumar Biradha for performing the single-crystal X-ray diffraction studies.

[1] For reviews see: a) M. J. Zaworotko, *Chem. Soc. Rev.* **1994**, *23*, 283–288; b) C. Janiak, *Angew. Chem.* **1997**, *109*, 1499–1502; *Angew. Chem. Int. Ed. Engl.* **1997**, *36*, 1431–1434; c) S. R. Batten, R. Robson, *Angew. Chem.* **1998**, *110*, 1558–1595; *Angew. Chem. Int. Ed.* **1998**, *37*, 1460–1494; d) P. J. Hagrman, D. Hagrman, J. Zubieta, *Angew. Chem.* **1999**, *111*, 2798–2848; *Angew. Chem. Int. Ed.* **1999**, *38*, 2638–2684; e) A. K. Cheetham, G. Férey, T. Loiseau, *Angew. Chem.* **1999**, *111*, 3466–3492; *Angew. Chem. Int. Ed.* **1999**, *38*, 3268–3292; f) A. J. Blake, N. R. Champness, P. Hubberstey, W.-S. Li, M. A. Withersby, M. Schröder, *Coord. Chem. Rev.* **1999**, *183*, 117–138; g) R. Robson, *J. Chem. Soc. Dalton Trans.* **2000**, 3735–3744; h) M. O'Keeffe, M. Eddaoudi, H. Li, T. Reineke, O. M. Yaghi, *J. Solid State Chem.* **2000**, *152*, 3–20; i) M. J. Zaworotko, *Chem. Commun.* **2001**, 1–9; j) B. Moulton, M. J. Zaworotko, *Chem. Rev.* **2001**, *101*, 1629–1658; k) G. Férey, *Chem. Mater.* **2001**, *13*, 3084–3098; l) B. Moulton, M. J. Zaworotko, *Curr. Opin. Solid State Mater. Sci.* **2002**, *6*, 117–123; m) S. A. Barnett, N. R. Champness, *Coord. Chem. Rev.* **2003**, *246*, 145–168; n) O. M. Yaghi, M. O'Keeffe, N. W. Ockwig, H. K. Chae, M. Eddaoudi, J. Kim, *Nature* **2003**, *423*, 705–714; o) C. Janiak, *Dalton Trans.* **2003**, 2781–2804; p) S. L. James, *Chem. Soc. Rev.* **2003**, *32*, 276–288.

[2] a) O. M. Yaghi, *Access in Nanoporous Materials* **1995**, 111–121; b) O. M. Yaghi, H. Li, C. Davis, D. Richardson, T. L. Groy, *Acc. Chem. Res.* **1998**, *31*, 474–484; c) S. Kitagawa, M. Kondo, *Bull. Chem. Soc. Jpn.* **1998**, *71*, 1739–1753; d) O. Kahn, *Acc. Chem. Res.* **2000**, *33*, 647–657; e) I. Goldberg, *Chem. Eur. J.* **2000**, *6*, 3863–3870; f) S. Feng, R. Xu, *Acc. Chem. Res.* **2001**, *34*, 239–247; g) M. Eddaoudi, D. B. Moler, H. Li, B. Chen, T. M. Reineke, M. O'Keeffe, O. M. Yaghi, *Acc. Chem. Res.* **2001**, *34*, 319–330; h) N. L. Rosi, M. Eddaoudi, J. Kim, M. O'Keeffe, O. M. Yaghi, *CrystEngComm* **2002**, *4*, 401–404.

[3] a) W. Lin, Z. Wang, L. Ma, *J. Am. Chem. Soc.* **1999**, *121*, 11249–11250; b) M.-C. Brandys, R. J. Puddephatt, *J. Am. Chem. Soc.* **2001**, *123*, 4839–4840; c) J. Zhang, M. M. Matsushita, X. X. Kong, J. Abe, T. Iyoda, *J. Am. Chem. Soc.* **2001**, *123*, 12105–12106.

[4] a) J. A. Real, E. Andrés, M. C. Muñoz, M. Julve, T. Granier, A. Bousseksou, F. Varret, *Science* **1995**, *268*, 265–267; b) E. Coronado, J. R. Galán-Mascarós, C. J. Gómez-Garcia, V. Laukhin, *Nature* **2000**, *408*, 447–449; c) M. Monfort, I. Resino, J. Ribas, H. Stoeckli-Evans, *Angew. Chem.* **2000**, *112*, 197–199; *Angew. Chem. Int. Ed.* **2000**, *39*, 191–193; d) W. Lin, O. R. Evans, G. T. Yee, *J. Solid State Chem.* **2000**, *152*, 152–158; e) B.-Q. Ma, S. Gao, G. Su, G.-X. Xu, *Angew. Chem.* **2001**, *113*, 448–451; *Angew. Chem. Int. Ed.* **2001**, *40*, 434–437; f) W. Fujita, K. Awaga, *J. Am. Chem. Soc.* **2001**, *123*, 3601–3602; g) G. Ballester, E. Coronado, C. Giménez-Saiz, F. M. Romero, *Angew. Chem.* **2001**, *113*, 814–817; *Angew. Chem. Int. Ed.* **2001**, *40*, 792–795; h) G. J. Halder, C. J. Kepert, B. Moubaraki, K. S. Murray, J. D. Cashion, *Science* **2002**, *298*, 1762–1765; i) J. C. Noveron, M. S. Lah, R. E. Del Sesto, A. M. Arif, J. S. Miller, P. J. Stang, *J. Am. Chem. Soc.* **2002**, *124*, 6613–6625; j) N. Usuki, M. Ohba, H. Okawa, *Bull. Chem. Soc. Jpn.* **2002**, *75*, 1693–1698; k) E.-Q. Gao, S.-Q. Bai, Z.-M. Wang, C.-H. Yan, *J. Am. Chem. Soc.* **2003**, *125*, 4984–4985; l) A. Galet, V. Niel, M. C. Muñoz, J. A. Real, *J. Am. Chem. Soc.* **2003**, *125*, 14224–14225.

[5] a) W. Su, M. Hong, J. Weng, R. Cao, S. Lu, *Angew. Chem.* **2000**, *112*, 3033–3036; *Angew. Chem. Int. Ed.* **2000**, *39*, 2911–2914; b) C. N. R. Rao, A. Ranganathan, V. R. Pedireddi, A. R. Raju, *Chem. Commun.* **2000**, 39–40.

[6] a) B. F. Abrahams, B. F. Hoskins, D. M. Michail, R. Robson, *Nature* **1994**, *369*, 727–729; b) G. B. Gardner, D. Venkataraman, J. S. Moore, S. Lee, *Nature* **1995**, *374*, 792–795; c) H. J. Choi, M. P. J. Suh, *J. Am. Chem. Soc.* **1998**, 120, 10622–10628; d) S. S.-Y. Chui, S. M.-F. Lo, J. P. H. Charmant, A. G. Orpen, I. D. Williams, *Science*

1999, *283*, 1148–1150; e) Y.-H. Kiang, G. B. Gardner, S. Lee, Z. Xu, E. B. Lobkovsky, *J. Am. Chem. Soc.* **1999**, *121*, 8204–8215; f) M. Eddaoudi, J. Kim, M. O'Keeffe, O. M. Yaghi, *J. Am. Chem. Soc.* **2002**, *124*, 376–377; g) C. Serre, F. Millange, C. Thouvenot, M. Noguès, G. Marsolier, D. Louër, G. Férey, *J. Am. Chem. Soc.* **2002**, *124*, 13519–13526.

[7] a) M. Kondo, T. Yoshitomi, K. Seki, H. Matsuzaka, S. Kitagawa, *Angew. Chem.* **1997**, *109*, 1844–1846; *Angew. Chem. Int. Ed. Engl.* **1997**, *36*, 1725–1727; b) H. Li, M. Eddaoudi, T. L. Groy, O. M. Yaghi, *J. Am. Chem. Soc.* **1998**, *120*, 8571–8572; c) H. Li, M. Eddaoudi, M. O'Keeffe, O. M. Yaghi, *Nature* **1999**, *402*, 276–279; d) M. Kondo, T. Okubo, A. Asami, S. Noro, T. Yoshitomi, S. Kitagawa, T. Ishii, H. Matsuzaka, K. Seki, *Angew. Chem.* **1999**, *111*, 190–193; *Angew. Chem. Int. Ed.* **1999**, *38*, 140–143; e) C. J. Kepert, M. J. Rosseinsky, *Chem. Commun.* **1999**, 375–376; f) B. Chen, M. Eddaoudi, S. T. Hyde, M. O'Keeffe, O. M. Yaghi, *Science* **2001**, *291*, 1021–1023; g) D. Li, K. Kaneko, *Chem. Phys. Lett.* **2001**, *335*, 50–56; h) A. J. Fletcher, E. J. Cussen, T. J. Prior, M. J. Rosseinsky, C. J. Kepert, K. M. Thomas, *J. Am. Chem. Soc.* **2001**, *123*, 10001–10011; i) K. Seki, *Chem. Commun.* **2001**, 1496–1497; j) M. Eddaoudi, J. Kim, N. Rosi, D. Vodak, J. Wachter, M. O'Keeffe, O. M. Yaghi, *Science* **2002**, *295*, 469–472; k) R. Kitaura, S. Kitagawa, Y. Kubota, T. C. Kobayashi, K. Kindo, Y. Mita, A. Matsuo, M. Kobayashi, H.-C. Chang, T. C. Ozawa, M. Suzuki, M. Sakata, M. Takata, *Science* **2002**, *298*, 2358–2361; l) E. J. Cussen, J. B. Claridge, M. J. Rosseinsky, C. J. Kepert, *J. Am. Chem. Soc.* **2002**, *124*, 9574–9581; m) K. Uemura, S. Kitagawa, M. Kondo, K. Fukui, R. Kitaura, H.-C. Chang, T. Mizutani, *Chem. Eur. J.* **2002**, *8*, 3586–3600; n) K. Seki, W. Mori, *J. Phys. Chem. B* **2002**, *106*, 1380–1385; o) N. L. Rosi, J. Eckert, M. Eddaoudi, D. T. Vodak, J. Kim, M. O'Keeffe, O. M. Yaghi, *Science* **2003**, *300*, 1127–1129; p) P. M. Forster, J. Eckert, J.-S. Chang, S.-E. Park, G. Férey, A. K. Cheetham, *J. Am. Chem. Soc.* **2003**, *125*, 1309–1312; q) R. Kitaura, K. Seki, G. Akiyama, S. Kitagawa, *Angew. Chem.* **2003**, *115*, 444–447; *Angew. Chem. Int. Ed.* **2003**, *42*, 428–431; r) L. Pan, H. Liu, X. Lei, X. Huang, D. H. Olson, N. J. Turro, J. Li, *Angew. Chem.* **2003**, *115*, 560–564; *Angew. Chem. Int. Ed.* **2003**, *42*, 542–546; s) S. Takamizawa, E. Nakata, H. Yokoyama, K. Mochizuki, W. Mori, *Angew. Chem.* **2003**, *115*, 4467–4470; *Angew. Chem. Int. Ed.* **2003**, *42*, 4331–4334.

[8] a) O. M. Yaghi, G. Li, H. Li, *Nature* **1995**, *378*, 703–706; b) D. Venkataraman, G. B. Gardner, S. Lee, J. S. Moore, *J. Am. Chem. Soc.* **1995**, *117*, 11600–11601; c) O. M. Yaghi, C. E. Davis, G. Li, H. Li, *J. Am. Chem. Soc.* **1997**, *119*, 2861–2868; d) H. J. Choi, T. S. Lee, M. P. Suh, *Angew. Chem.* **1999**, *111*, 1490–1493; *Angew. Chem. Int. Ed.* **1999**, *38*, 1405–1408; e) K. Kasai, M. Aoyagi, M. Fujita, *J. Am. Chem. Soc.* **2000**, *122*, 2140–2141; f) K. Biradha, Y. Hongo, M. Fujita, *Angew. Chem.* **2000**, *112*, 4001–4003; *Angew. Chem. Int. Ed.* **2000**, *39*, 3843–3845; g) Y.-B. Dong, M. D. Smith, H.-C. zur Loye, *Angew. Chem.* **2000**, *112*, 4441–4443; *Angew. Chem. Int. Ed.* **2000**, *39*, 4271–4273; h) F. M. Tabellion, S. R. Seidel, A. M. Arif, P. J. Stang, *Angew. Chem.* **2001**, *113*, 1577–1580; *Angew. Chem. Int. Ed.* **2001**, *40*, 1529–1532; i) C.-Y. Su, X.-P. Yang, B.-S. Kang, T. C. W. Mak, *Angew. Chem.* **2001**, *113*, 1775–1778; *Angew. Chem. Int. Ed.* **2001**, *40*, 1725–1728; j) K. S. Min, M. P. Suh, *Chem. Eur. J.* **2001**, *7*, 303–313; k) S. K. Mäkinen, N. J. Melcer, M. Parvez, G. K. H. Shimizu, *Chem. Eur. J.* **2001**, *7*, 5176–5182; l) K. Biradha, M. Fujita, *Chem. Commun.* **2001**, 15–16; m) K. Biradha, M. Fujita, *Angew. Chem.* **2002**, *114*, 3542–3545; *Angew. Chem. Int. Ed.* **2002**, *41*, 3392–3395; n) K. Biradha, Y. Hongo, M. Fujita, *Angew. Chem.* **2002**, *114*, 3545–3548; *Angew. Chem. Int. Ed.* **2002**, *41*, 3395–3398.

[9] a) B. F. Hoskins, R. Robson, *J. Am. Chem. Soc.* **1990**, *112*, 1546–1554; b) O. M. Yaghi, H. Li, *J. Am. Chem. Soc.* **1996**, *118*, 295–296; c) K. S. Min, M. P. Suh, *J. Am. Chem. Soc.* **2000**, *122*, 6834–6840.

[10] a) M. Fujita, Y. J. Kwon, S. Washizu, K. Ogura, *J. Am. Chem. Soc.* **1994**, *116*, 1151–1152; b) T. Sawaki, T. Dewa, Y. Aoyama, *J. Am. Chem. Soc.* **1998**, *120*, 8539–8540; c) J. S. Seo, D. Whang, H. Lee, S. I. Jun, J. Oh, Y. J. Jeon, K. Kim, *Nature* **2000**, *404*, 982–986.

[11] T. L. Hennigar, D. C. MacQuarrie, P. Losier, R. D. Rogers, M. J. Zaworotko, *Angew. Chem.* **1997**, *109*, 1044–1046; *Angew. Chem. Int. Ed. Engl.* **1997**, *36*, 972–973.

[12] a) F. M. Tabellion, S. R. Seidel, A. M. Arif, P. J. Stang, *Angew. Chem.* **2001**, *113*, 1577–1580; *Angew. Chem. Int. Ed.* **2001**, *40*, 1529–1532; b) F. M. Tabellion, S. R. Seidel, A. M. Arif, P. J. Stang, *J. Am. Chem. Soc.* **2001**, *123*, 11982–11990.

[13] M. Fujita, Y. J. Kwon, O. Sasaki, K. Yamaguchi, K. Ogura, *J. Am. Chem. Soc.* **1995**, *117*, 7287–7288.

[14] O.-S. Jung, S. H. Park, D. C. Kim, K. M. Kim, *Inorg. Chem.* **1998**, *37*, 610–611.

[15] M. J. Plater, M. R. St. J. Foreman, T. Gelbrich, S. J. Coles. M. B. Hursthouse, *J. Chem. Soc. Dalton Trans.* **2000**, 3065–3073.

[16] M. J. Plater, M. R. St. J. Foreman, R. A. Howie, J. M. S. Skakle, *Inorg. Chim. Acta* **2000**, *318*, 175–180.

[17] S. Konar, E. Zangrando, M. G. B. Drew, T. Mallah, J. Ribas, N. R. Chaudhuri, *Inorg. Chem.* **2003**, *42*, 5966–5973.

[18] M. Fujita, O. Sasaki, K. Watanabe, K. Ogura, K. Yamaguchi, *New J. Chem.* **1998**, *22*, 189–191.

[19] C. R. Patrick, G. S. Prosser, *Nature*, **1960**, *187*, 1021.

[20] a) J. H. Williams, *Acc. Chem. Res.* **1993**, *26*, 593–598; b) G. W. Coates, A. R. Dunn, L. M. Henling, D. A. Dougherty, R. H. Grubbs, *Angew. Chem.* **1997**, *109*, 290–293; *Angew. Chem. Int. Ed. Engl.* **1997**, *36*, 248–251; c) F. Ponzini, R. Zagha, K. Hardcastle, J. S. Siegel, *Angew. Chem.* **2000**, *112*, 2413–2415; *Angew. Chem. Int. Ed.* **2000**, *39*, 2323–2325; d) W. J. Feast, P. W. Lövenich, H. Puschmann, C. Taliani, *Chem. Commun.* **2001**, 505–506; e) E. A. Meyer, R. K. Castellano, F. Diederich, *Angew. Chem.* **2003**, *115*, 1244–1287; *Angew. Chem. Int. Ed.* **2003**, *42*, 1210–1250; f) K. Reichenbächer, H. I. Süss, J. Hulliger, *Chem. Soc. Rev.* **2005**, *34*, 22–30.

[21] a) V. R. Thalladi, H.-C. Weiss, D. Bläser, R. Boese, A. Nangia, G. R. Desiraju, *J. Am. Chem. Soc.* **1998**, *120*, 8702–8710; b) V. R. Vangala, A. Nangia, V. M. Lynch, *Chem. Commun.* **2002**, 1304–1305.

Received: August 31, 2005
Revised: July 7, 2006
Published online: January 3, 2007

